

CHARACTERIZATION OF EARTHQUAKE SHAKING EFFECTS

1. Introduction

This section presents information on engineering seismology and engineering characterization of earthquakes. The key references for this module are Bolt (1988), Bozorgnia and Bertero (2004), FEMA (2004), Kramer (1996), SRL (1997) and McGuire (2004). The objective of this lecture is to introduce the reader to

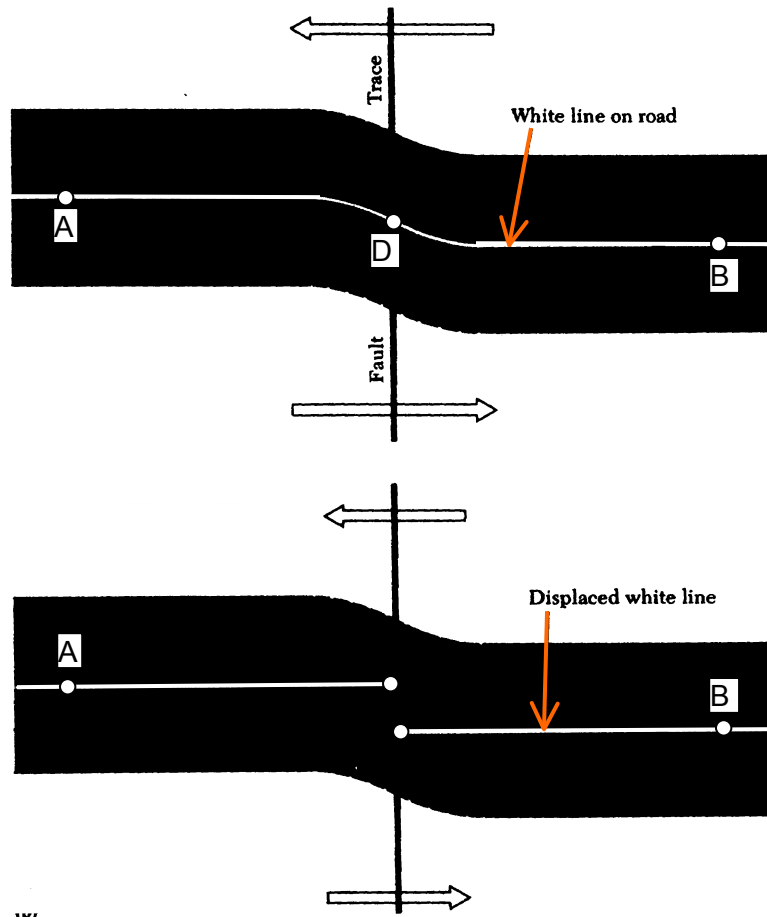
- Basic concepts and terminology in seismology
- Factors that influence earthquake shaking at a site
- Characterization of earthquakes for structural engineers
- Attenuation relationships
- Seismic hazard analysis
- Hazard characterization per the 2003 *NEHRP Recommended Provisions* (FEMA 2004).
- New developments in the 2010 ASCE 7

2. Basic Concepts in Seismology

2.1 Elastic Rebound Theory

The elastic rebound theory proposes that as two plates move relative to the other along a fault segment, elastic strain energy develops in the rock along the plate boundaries, and that *rupture* occurs once the shear stresses in the rock exceed the shear strength of the rock. This is illustrated in the figure below from Bolt (1988). Because fault planes are generally highly fractured, substantial strain energy can be stored before rupture. If the shear strength of the plate boundary is known, the length of the fault is known, the rate at which the plates are moving relative to one another (termed the slip rate) is known, the time required to build up sufficient strain energy to produce an earthquake and the probable magnitude of that earthquake can be *estimated*.

The illustration of Bolt is of a road running at right angles to the fault. Immediately following construction of the road, the line (**ADB**) is straight. After time, the line bends with the left side moving with respect to the right side, with the deformation constrained to a relatively narrow width (10s to 100s of meters). Once the strength threshold of the interface is reached, the fault ruptures and each side of the fault rebounds, that is, point **D** moves to **D₁** on the left-hand-side of the fault and **D₂** on the right-hand-side of the fault.



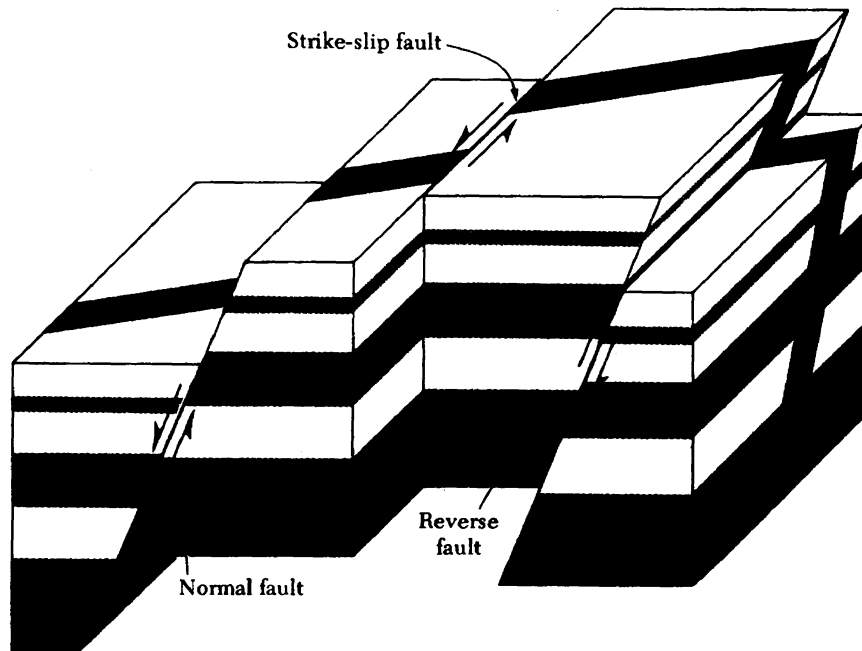
The figure below shows the effect of fault rupture on a farm fence following the 1906 San Francisco earthquake.



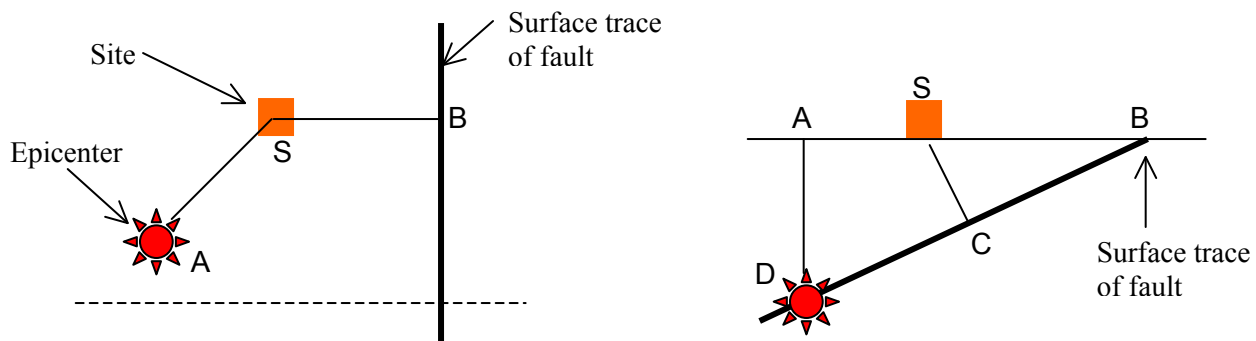
2.2 Faulting

Following Bolt, fault displacements can be classified into one of two types: *strike-slip* and *dip-slip*. The figure on the following page from Bolt illustrates strike slip and dip-slip (normal and reverse) faulting. Faulting is often a combination of strike-slip and dip-slip.

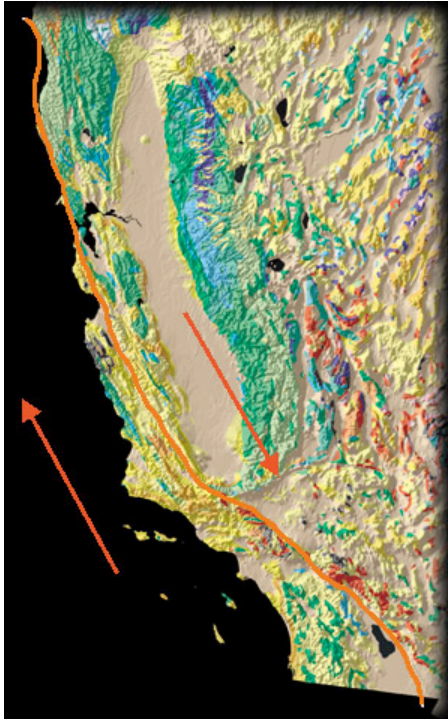
- *Strike-slip*
 - Faulting that produces only *horizontal* displacements along the strike of the fault
 - ◆ The direction from north of the line of the plane of the fault at the surface is termed the *strike*.
 - ◆ The arrows on the strike-slip fault below show left-lateral faulting. To determine whether the fault is *left-lateral* or *right-lateral*, imagine that you are standing on one side of the fault line looking across the fault. If the offset on the other side of the fault line is from right to left, the faulting is *left-lateral*. Vice-versa for the other direction.
- *Dip-slip*
 - Faulting that produces *vertical* displacements along the strike of the fault
 - ◆ 90° dip is vertical
 - Two types of dip-slip faults: *normal* fault and *reverse* fault
 - ◆ *Normal* fault: when the rock on that side of the fault hanging over fracture (the *hanging wall*) plane slips downward
 - ◆ *Reverse* fault: when the hanging wall moves upwards over the footwall.
 - A *thrust* fault is a special type of reverse fault in which the dip of the fault is small (shallow). Subduction zones (e.g., Cascadia in the Pacific North West) are the sites of many *thrust* earthquakes.



The distance from the site of a building or recording station to the fault or fault projection is described by a number of terms, which are illustrated below: SA = epicentral distance; SB = distance to fault rupture; CD = hypocentral distance or slant distance; and SC = distance to rupture.



The best-known fault in the United States is the San Andreas Fault in California. Information on the fault and others in the United States is available at a number of web sites including those of the Southern California Earthquake Center (SCEC) at www.scec.org, the California Geological Survey at www.consrv.ca.gov and the United States Geological Survey (USGS) at www.usgs.gov. Consider the image on the following page that shows the extent of the San Andreas Fault. This fault is composed of many segments or combinations of segments: 14 by the count of USGS, with various slip rates, maximum moment magnitudes and return periods.



- Pacific plate sliding against ???
- Fault type is ?????
- Length of 1200 km
- Fault zone width up to 1 km
- Part of plate motion is compressional
 - Los Angeles basin
- Last major ruptures
 - January 1857, Mojave segment
 - April 1906, Northern segment
- Slip rate: 20 to 35 mm per year
- Intervals between ruptures
 - 140 years on Mojave segment
- Probable magnitudes: M_W 6.8 to 8.0

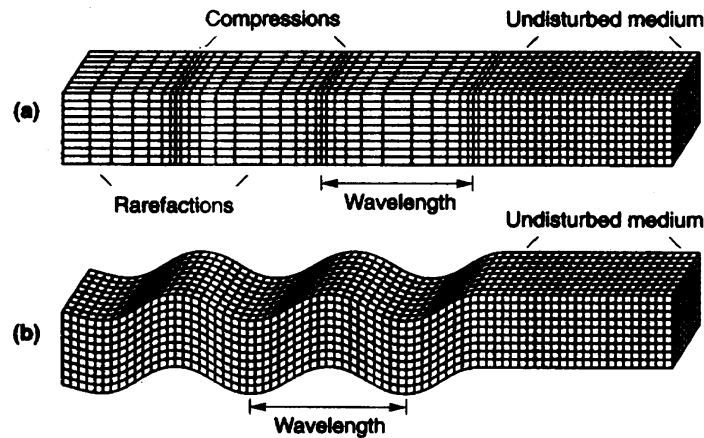
A good understanding of the fault sources, slip rates, geologic conditions and historical seismicity (written record and trenching) is needed to perform a robust seismic hazard assessment. Seismic hazard assessment, both deterministic and probabilistic, is discussed later in this lecture.

2.3 Seismic Wave Propagation

A detailed presentation on seismic wave propagation is beyond the scope of this lecture. Details can be found in Bolt (1998), Bozorgnia and Bertero (2004) and Kramer (1996). Seismic waves are parsed into two types, namely, body waves and surface waves. Summary information only is presented below in a bulleted list.

- Body waves
 - P waves: compression waves, generally not damaging; (a) below from Kramer
 - S waves: shear waves, cause damage to structures; (b) below from Kramer
 - ◆ SV-wave particle motions in the vertical plane; SH-wave particle motion in the horizontal plane
 - Geologic materials stiffest in compression; P waves travel faster than S waves and arrive first at a site
 - ◆ P waves: velocity ~ 5 km/sec. in hard rock; 1.5 km/sec. in water

- ◆ S waves: velocity ~ 3 km/sec. in hard rock; 0 km/sec. in water (no shear stiffness)



- Surface waves
 - Result from interaction between the body waves and the surface and surficial layers of the earth
 - Travel along the earth's surface with amplitudes that decrease with depth
 - Can dominate peak ground motions at distances greater than about twice the crust thickness (50 to 80 kms from the epicenter)
- ◆ Important?
 - *Raleigh* waves and *Love* waves

3. Earthquake Shaking

3.1 Introduction

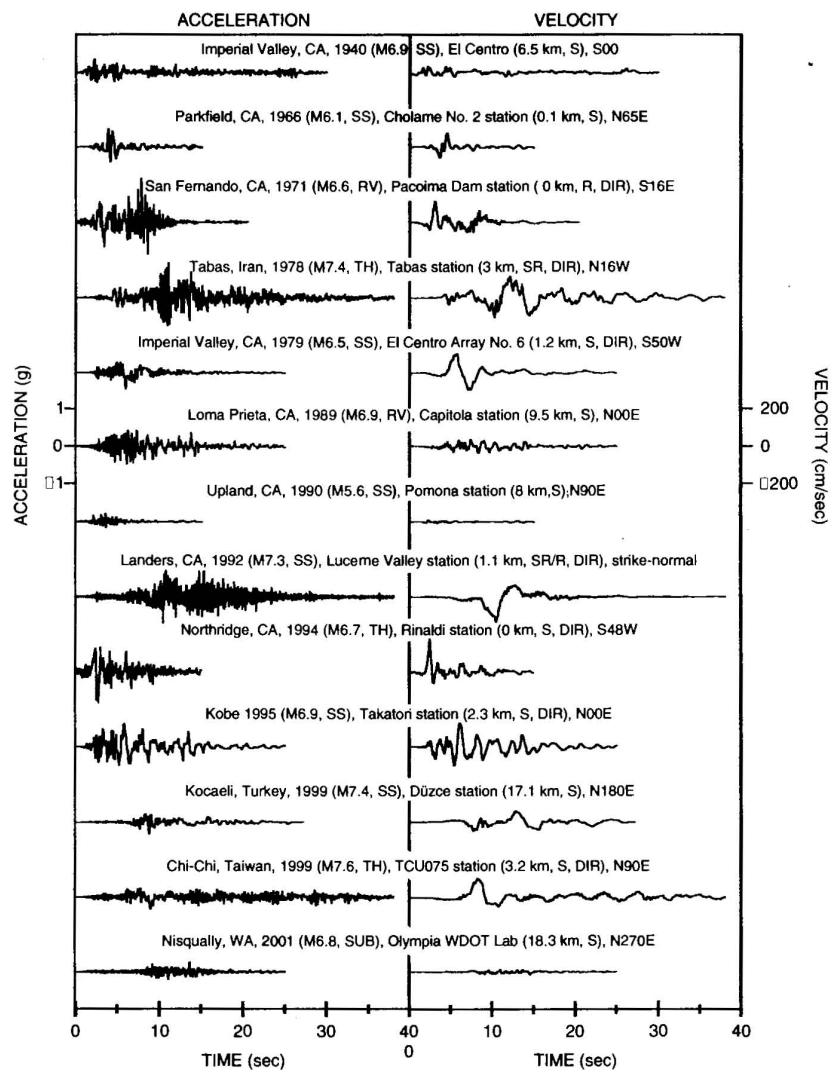
Earthquake-acceleration histories (time-series) or earthquake ground motions recorded during different earthquake sand at different sites will vary significant due to factors including

- Earthquake magnitude
- Source or faulting mechanism
- Travel path (source to site) and epicentral distance
- Site response
- Soil-structure interaction

- Proximity to the fault (near-source or near-fault)

3.2 Earthquake Histories

The figure shown below from Bozorgnia and Bertero (Eds., 2004) presents plots of earthquake acceleration histories dating back to 1940. These histories are plotted at the same scale. In this figure, the largest peak ground acceleration is 1.17 g for the 1971 San Fernando earthquake and the largest peak ground velocity is 178 cm/sec for the Rinaldi Receiving Station during the 1994 Northridge earthquake. Large peak velocity can be associated with a fling-step (coined by Bolt) displacement pulse. Large magnitude earthquakes generally produce long-duration earthquake shaking. Why?



3.3 Earthquake Source Mechanism

Fault type and fault rupture process influence earthquake shaking histories. The effect of fault type (strike-slip, normal, reverse) is captured for the purpose of analysis through attenuation relationships. The rupture process, which is a) continuous and regular, or b) multiple and irregular, will also influence shaking at a site. If the rupture process for a site is well known, the process can be included in a seismic hazard analysis through the magnitude-recurrence relationship.

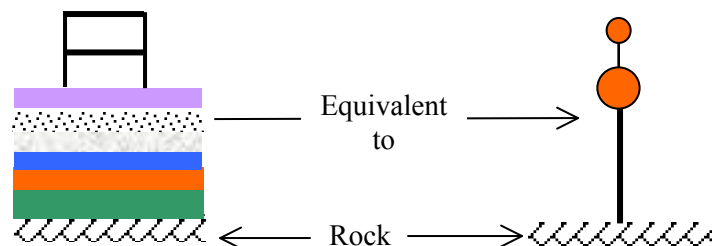
3.4 Epicentral Distance

Setting aside local soil conditions and basin effects, earthquake shaking attenuates with distance from the epicenter of the earthquake. Such a relationship between shaking intensity (acceleration, velocity, etc) is captured through attenuation relationships. For small epicentral distances (near-fault) and moderate-to-large magnitude earthquakes, earthquake histories might contain significant pulses. Such pulses are described later in this lecture.

3.5 Site Effects

Site effects include local ground-response effects, basin effects and the influence of surface topography on ground motion.

- Local ground response refers to the influence of relatively shallow geologic materials on vertically propagating seismic waves. The soil column beneath a structure (setting aside basin effects at this time) responds as a dynamic (nonlinear) oscillator as follows:



Softer and/or deeper soil deposits will have shorter (or longer) predominant frequency content?

Local site effects on structural response can be captured using the full soil profile (from ground surface to bedrock) but for sites with very deep sediments, the soil models do not extend below the upper 100 m. Much work on site classification and soil amplification was conducted in the United States following the 1989 Loma Prieta earthquake.

- Yerba Buena and Treasure Islands, 100 km from the epicenter of the earthquake.

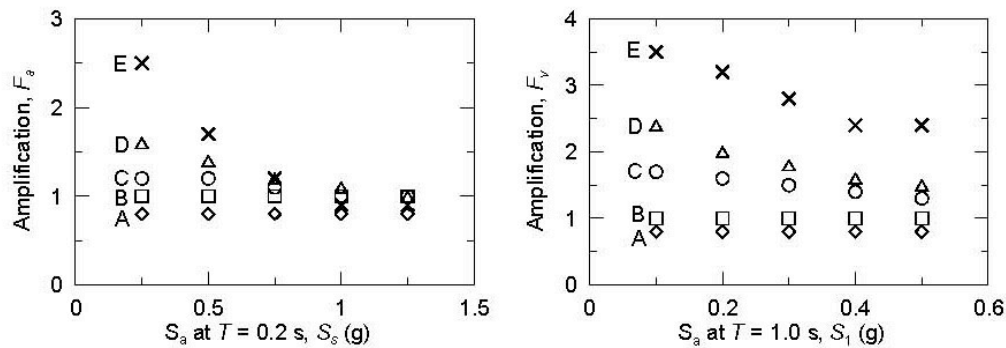
- Basin effects refer to the influence of two- or three-dimensional sedimentary basin structures on ground motions, including body wave reflections and surface wave generation at basin edges. A short presentation on basin effects is presented in Chapter 4 of Bozorgnia and Bertero (2004).
- Topographic effects can amplify ground motion shaking that would otherwise be expected on level ground along ridges or near the tops of slopes. Similarly, the intensity of ground-motion shaking can be reduced due to topographical effects in canyons or at the base of slopes.

Recorded earthquake histories vary widely in amplitude, frequency content and duration. Record-to-record variability between stations is often high, even for a given earthquake (M) and distance (r), due in many cases to local soil conditions. A number of schemes have been proposed in the United States to classify the soil type at a given site. The most widely used classification scheme is the averaged shear-wave velocity in the upper 30 m of the soil column: based in part on work done in the mid 1960s, which suggested that ground-motion amplitude was affected most by shear-wave velocity and soil density in the near-surface soil deposits. This classification scheme is used in the 2003 *NEHRP Recommended Provisions*, which classify soils in categories A through F. The table below, which is adapted from Chapter 4 the 2003 *NEHRP Recommended Provisions*, presents shear-wave velocities for the 6 categories. (Undrained shear strength and averaged standard penetration test data can also be used to classify sites.)

NEHRP Category	Description	Mean Shear-Wave Velocity to 30 m (m/sec)
A	Hard rock (East Coast)	>1500
B	Firm to hard rock (West Coast)	760-1500
C	Very dense soil, soft rock	360-760
D	Stiff soil	180-360
E	Soft clays	<180
F	Special study soils, liquefiable soils, highly sensitive clays, etc.	NA

Site amplification factors are used to capture the effects of local soil conditions on expected earthquake shaking at the ground surface at a site. In the 2003 *NEHRP Recommended Provisions*, site amplification factors are provided for the six NEHRP categories listed above and different levels of earthquake shaking, measured using spectral responses in the short-period (0.2 second) and long-period (1.0 second) ranges. The factors given in the tables in the *NEHRP*

Recommended Provisions represent the ratio of the spectral acceleration for a given site category in the *free field*¹ to the value of the parameter for a reference category, which is Category B (West Coast rock) in the *Provisions*. The figure below, which is adapted from the 2003 *NEHRP Recommended Provisions* and presented in Bozorgnia and Bertero (2004), shows the site factors (termed F_a and F_v in the *Provisions*) as a function of soil type and spectral acceleration. Values are tabulated in the *Provisions*. What conclusions can be drawn from these figures?

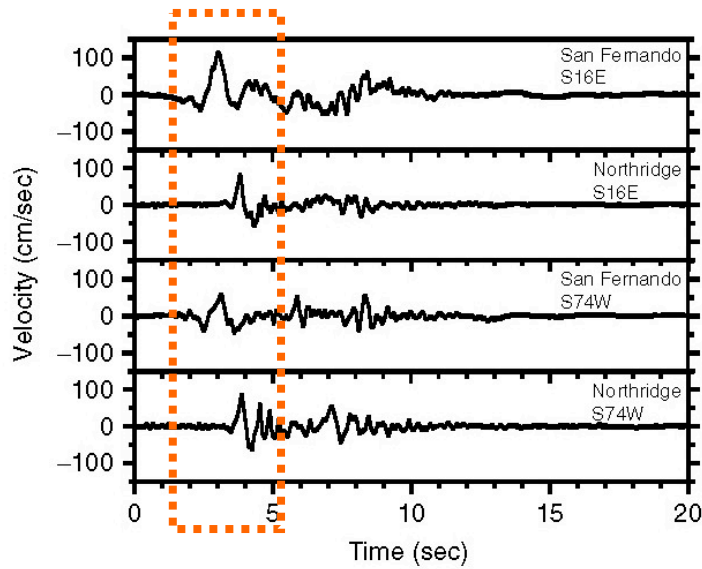


4.7 Near-Fault Effects

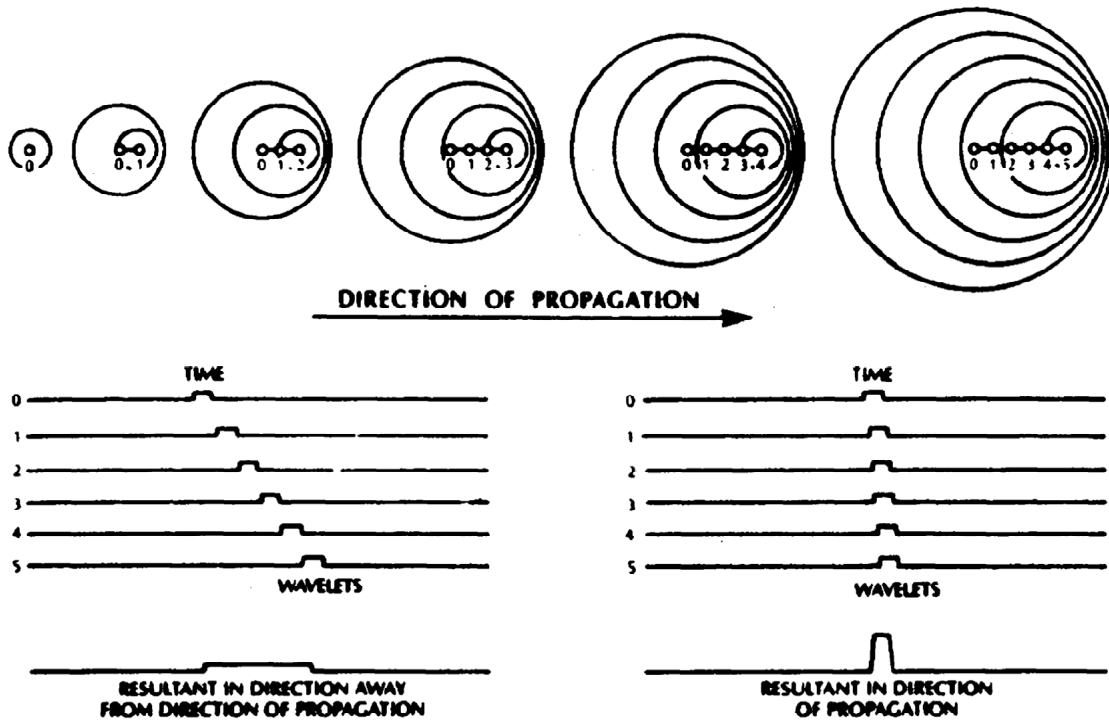
Earthquake shaking histories (ground motions) recorded close to faults during large-magnitude earthquakes often include significant single-sided or double-sided wave pulses with durations from 0.5 second to 4 seconds and greater. Such pulses were first observed following the 1971 San Fernando earthquake and analysis of earthquake histories recorded at Pacoima Dam. The figure below from Bozorgnia and Bertero (2004) presents the ground motion velocity pulses at Pacoima Dam during the 1971 San Fernando and 1994 Northridge earthquakes. In both cases, a large-velocity pulse is recorded near the beginning of the ground-motion record.

Two features of earthquake shaking create these long-period wave pulses: 1) constructive interference of the dynamic shaking due to the directivity of the fault rupture (termed the *directivity pulse*), and 2) movement of the ground associated with the permanent offset of the ground (*fling step*). Each of these effects is described in more detail below. Procedures for accounting for directivity effects in seismic hazard assessment have been developed by Somerville et al. (1997) and Abrahamson (2000) and these procedures are presented in the section of this lecture on attenuation relationships.

¹ Free-field motions are those motions not affected by structures, foundations, etc.



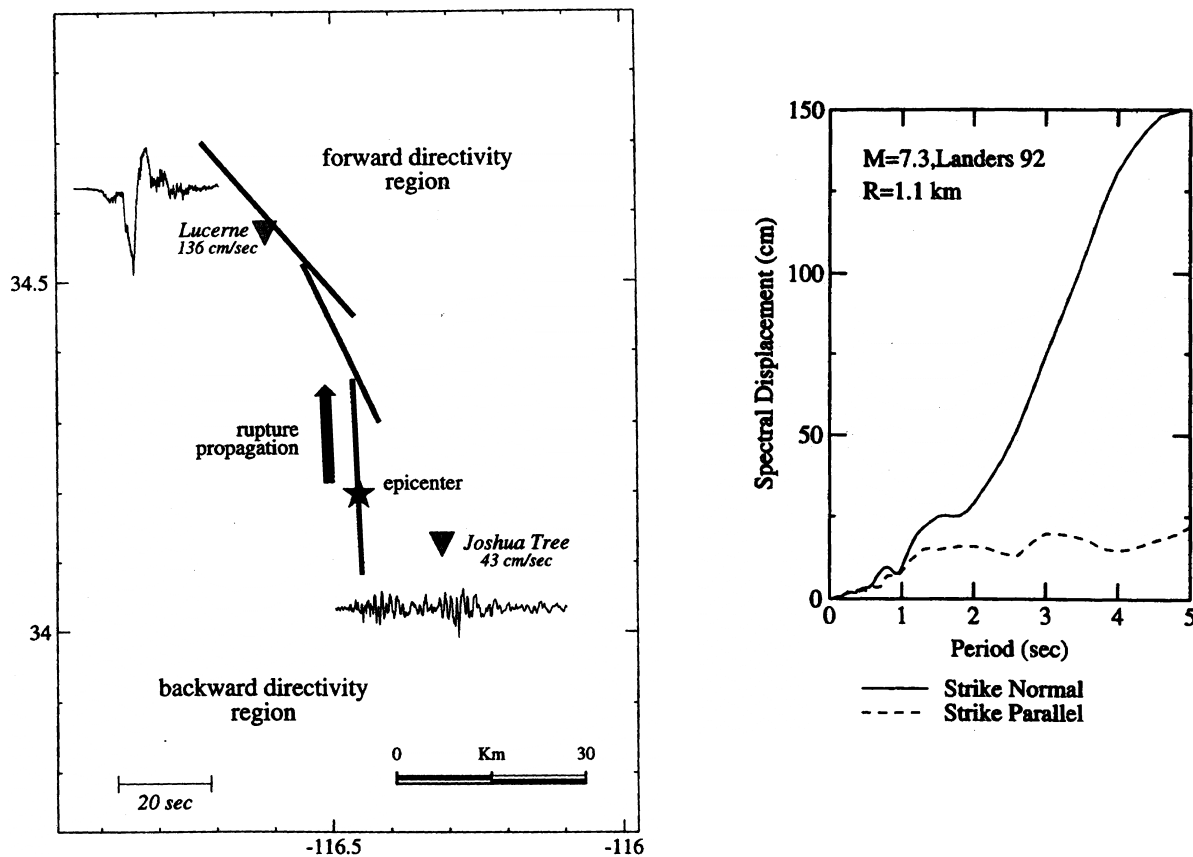
Singh (1985) and Bullen and Bolt (1985) each describe the physical mechanism for generating *directivity pulses*, which can be very significant if a fault ruptures toward a site or structure at *near constant velocity that is nearly as large as the shear wave velocity*. Consider the cartoon at the top of the following page from Singh (1985), which models the rupture as a series of point dislocations: 0, 1, 2, 3, 4, 5, and assume that the velocity of rupture is nearly as large as the shear wave velocity (= 2,500 ft/sec. to 5000 ft/sec for most rock).



There is a compression of the seismic wave front in the direction of propagation (left to right in the figure above) leading to

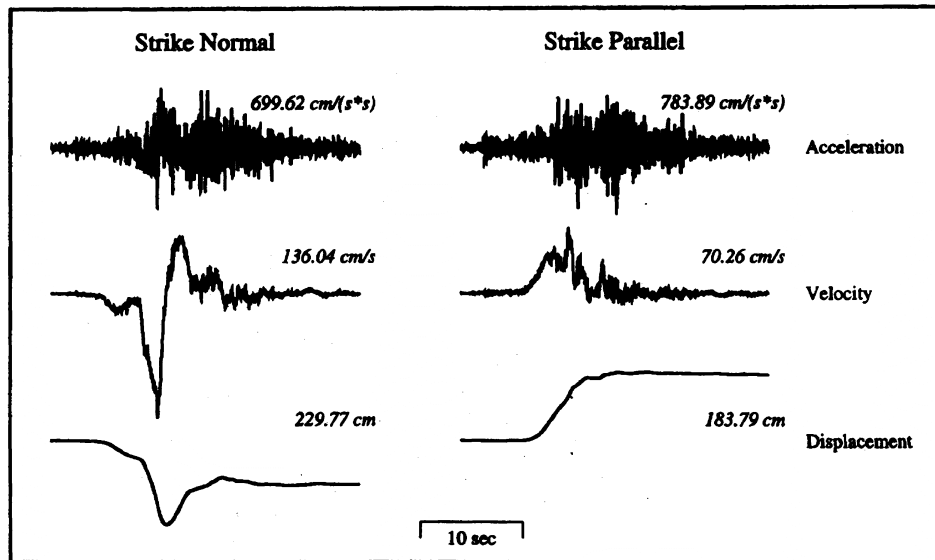
- Large intensity, short duration shaking in the forward azimuth direction, often characterized by a single large long-period pulse of velocity and displacement at the beginning of the ground-motion record
- Modest intensity, long duration shaking in the backward azimuth direction
- ??? at the point of rupture initiation.

The figures below from Somerville et al. (1997) illustrate the differences in ground motion (velocity histories) in the forward and backward azimuth directions. The data are from the 1992 Landers earthquake in Southern California, which was the earthquake that prompted many studies on the effects of near-fault shaking. What conclusions can be drawn from this figure?



As noted above, fault-rupture directivity causes spatial variations in the amplitude and duration of ground motion around faults and produces large differences between fault-normal and fault parallel components of horizontal ground motion amplitudes. See the figure to the right. Somerville, following analysis of 1999 Chi-Chi earthquake data showed that these differences

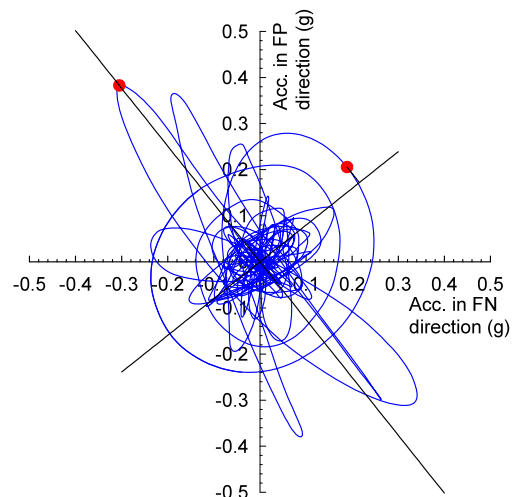
are bounded (unlike that shown in the spectrum to the right) and the peaks in the spectra are related to magnitude (and thus pulse period). The earthquake histories below from the Landers earthquake further illustrate the differences between fault-normal and fault-parallel ground motions.



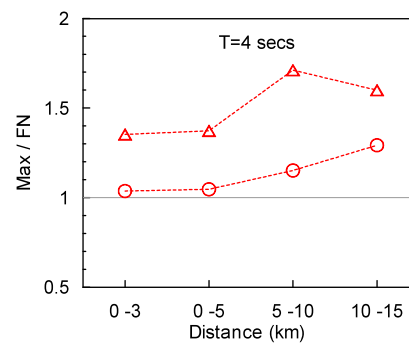
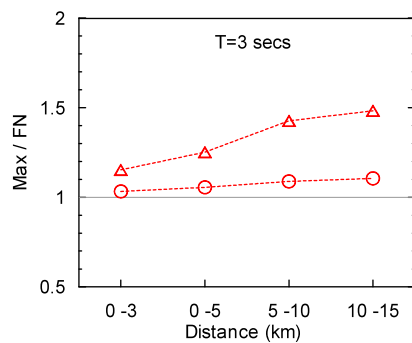
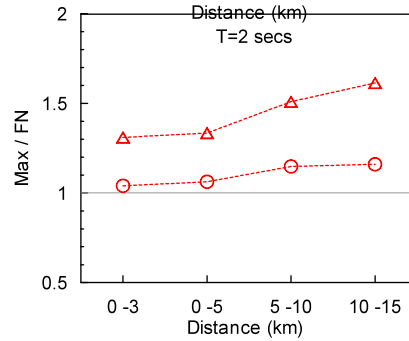
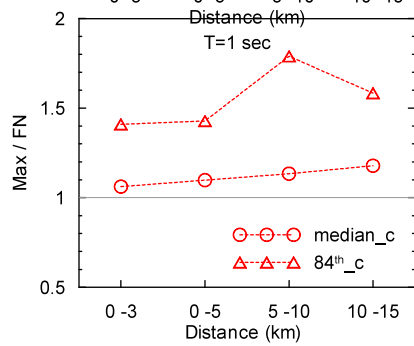
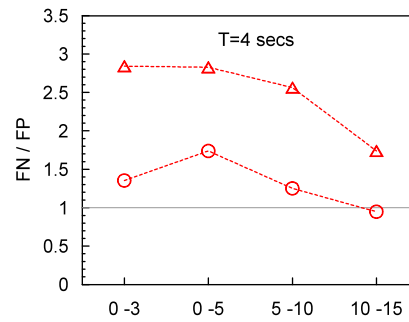
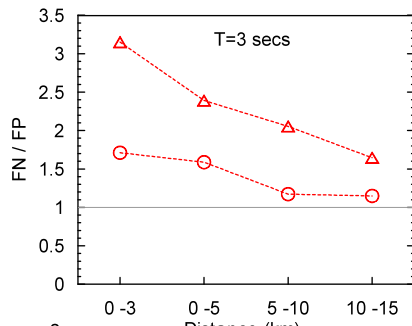
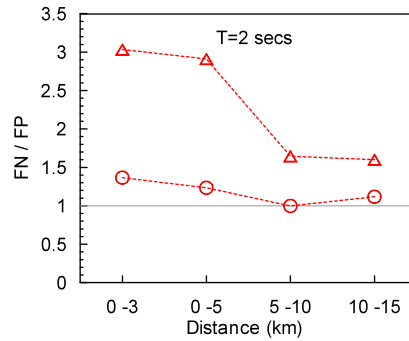
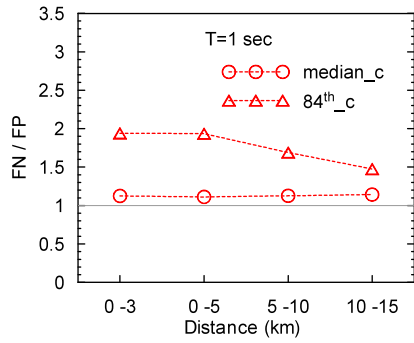
- Fault-normal direction: double-sided velocity pulse with no permanent displacement
- Fault-parallel direction: single-sided velocity pulse with a large permanent displacement

Fling step components of near-field pulses occur when the site is located close to a fault with significant surface rupture. The fling step occurs on the ground displacement component parallel to the slip direction as shown in the figure above. For strike-slip faults, the rupture directivity is observed on the fault-normal component and the (static) fling step is observed on the fault-parallel component. For dip slip faults, the resolution into rupture directivity and fling step components is more complex.

Huang et al. (2007) studied the relationship between fault-normal and maximum earthquake shaking in the near-fault region, assumed here to be less than 15 km from an active fault, using 147 near-fault records from the PEER database (www.peer.berkeley.edu). Maximum earthquake shaking was established in a spectral sense by rotating the two components (initially fault-normal and fault-parallel), one degree at a time, and computing spectral demands across a broad period range. See the figure to the right



that illustrates the calculation of the maximum spectral demand at a given period.



4. Characterizing Earthquakes Size Using Engineering Parameters

The size of an earthquake can be described in terms of *intensity*, *magnitude* and *energy* release. Each of these descriptors is introduced below.

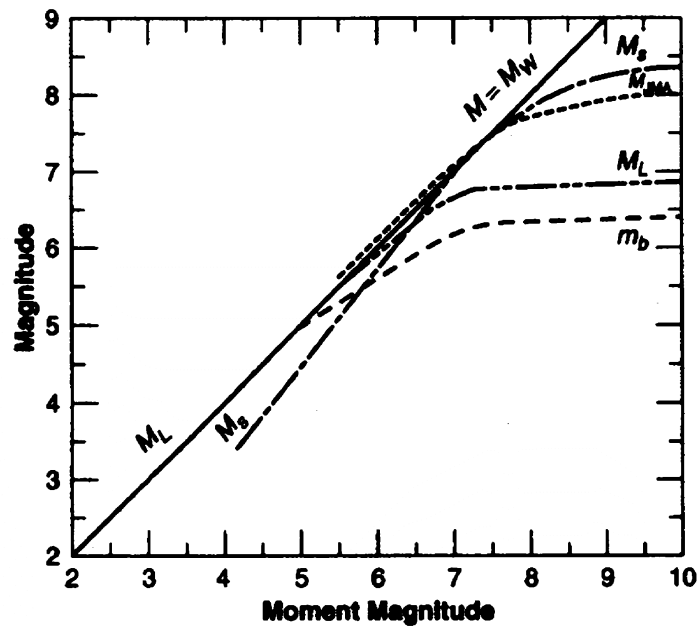
Earthquake intensity is a qualitative (and thus subjective) descriptor of the size of the earthquake and serves to record the level of damage and the response of people to the earthquake shaking. Intensity is

- Oldest measure of earthquake size
- Function of the distance from the epicenter or rupture plane.
- Intensity measures cannot be used for design.

Instruments such as the seismograph and accelerometer have made it possible to accurately measure earthquake ground motions. Several *magnitude* scales are used to report earthquakes but the best scale for scientific and engineering purposes is moment magnitude. The commonly used scales are listed below. Kramer provides much additional information.

M_L	Richter magnitude	Log of the pendulum displacement of a Wood-Anderson seismometer located 100 km from the epicenter. Traditional measure of magnitude.
M_W	Moment magnitude	Based on the seismic moment, M_0 , and is a measure of the work done by the rupture. $M_W = (\log_{10} M_0 / 1.5) - 10.7$, where $M_0 = \mu AD$, and μ is the rupture strength of the material along the fault, A is the rupture area, and D is the average amount of slip.
M_S	Surface wave magnitude	Amplitude of Raleigh waves with a period of 20 seconds. Used for distant earthquakes (>1000 km).
M_b	Body wave magnitude	Based on the amplitude of the first few cycles of P waves. Used for deep-focus earthquakes.

Ground-shaking characteristics do not proportionally increase with the total amount of energy released during an earthquake and some ground-motion measures saturate with magnitude. Only moment magnitude does not saturate as shown below in the figure from Kramer.



Wells and Coppersmith developed equations to relate magnitude and average displacement, maximum displacement, rupture area and subsurface rupture length. The equation to estimate the earthquake potential of a fault of a given length is:

$$M_W = a + b \log(SRL)$$

where SRL is the surface rupture length in kilometers and

<i>Fault type</i>	<i>a</i>	<i>b</i>
Strike slip	5.16	1.12
Normal	4.86	1.32
Reverse	5.00	1.22
All	5.08	1.16

The total seismic energy released during an earthquake is often estimated using the following equation:

$$\log_{10} E = 11.8 + 1.5M_S$$

where E is measured in ergs. A unit increase in magnitude corresponds to a $10^{1.5}$ or 32-fold increase in seismic energy.

5. Characterizing Earthquake Ground Motions Using Engineering Parameters

5.1 Introduction

Earthquake histories can be described using amplitude measures, frequency content, duration and spectra. Some of the well-established descriptors are introduced below. Additional information is presented in Kramer (1996) and Bozorgnia and Bertero (2004).

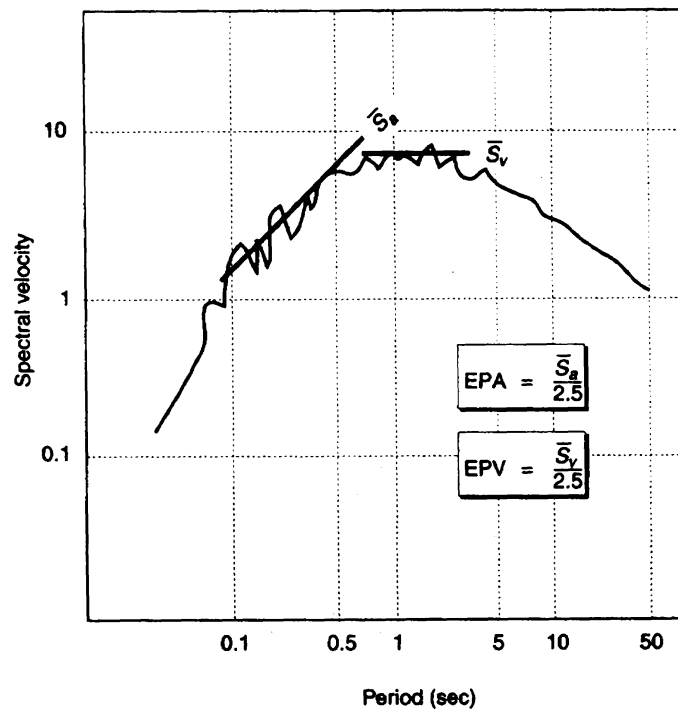
5.2 Amplitude

Common measures of shaking amplitude include

- Peak ground acceleration (PGA, ZPA, PHA, PVA)
- Effective peak acceleration (EPA): Newmark and Hall (1982), ATC-3-06 (1978)
- Peak ground velocity (PGV, PHV, PVV)
- Effective peak velocity (EPV)
- Peak ground displacement (PGD)

Effective peak acceleration and effective peak velocity are defined in the figure below.

- Are these definitions of amplitude better than peak ground acceleration?



5.3 Frequency Content

The frequency content of an earthquake history or earthquake ground motion is often described using Fourier Spectra, Power spectra, and response spectra. Details on the derivation of these spectra can be found in Kramer.

5.3.1 Fourier Spectra

A periodic function (for which an earthquake history [with a tail of zeros] is an approximation) can be written as

$$x(t) = c_0 + \sum_{n=1}^{\infty} c_n \sin(\omega_n t + \phi_n)$$

where c_n and ϕ_n are the *amplitude* and *phase angle*, respectively, of the n th harmonic in the Fourier series. The *Fourier amplitude spectrum* is a plot of c_n versus ω_n and shows how the motion varies with frequency.

The Fourier transform of a ground acceleration history $a_g(t)$ is defined as

$$\begin{aligned} F(\omega) &= \int_0^{T_0} a_g(t) e^{-i\omega t} d\omega \\ &= \int_0^{T_0} a_g(t) \cos \omega t d\omega - i \int_0^{T_0} a_g(t) \sin \omega t dt \\ &= C(\omega) - iS(\omega) \end{aligned}$$

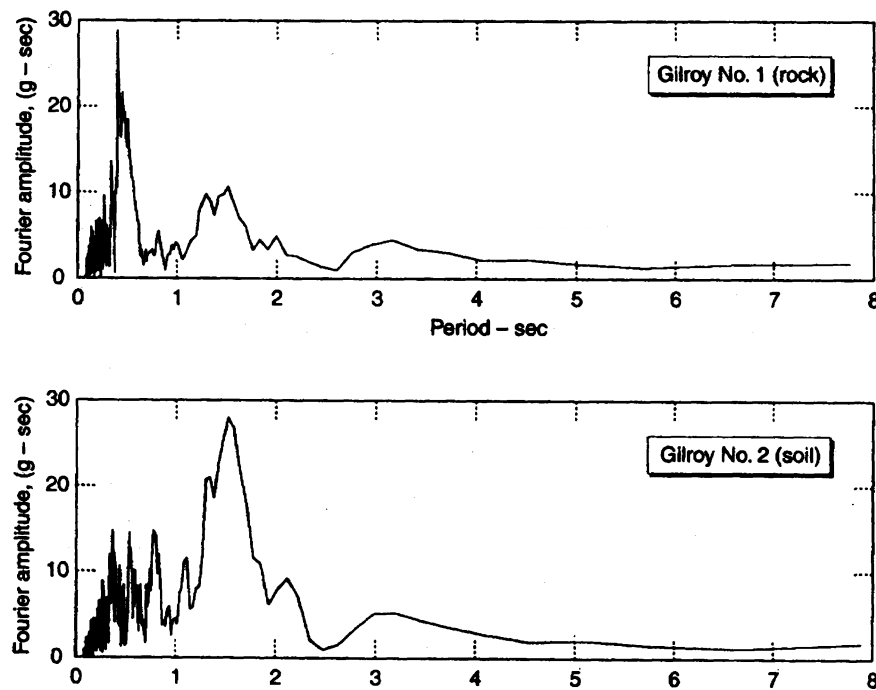
where ω is the circular frequency (rad/sec) and T_0 is the duration of the history. The Fourier transform $F(\omega)$ is a complex-valued function, which can be represented by its amplitude and phase angle. The Fourier amplitude spectrum $FAS(\omega)$ and Fourier phase spectrum $\Phi(\omega)$ are given by

$$\begin{aligned} FAS(\omega) &= \sqrt{C^2(\omega) + S^2(\omega)} \\ \Phi(\omega) &= -\tan^{-1} \left(\frac{S(\omega)}{C(\omega)} \right) \end{aligned}$$

Given the Fourier transform $F(\omega)$, the ground acceleration history can be recovered through the inverse Fourier transform:

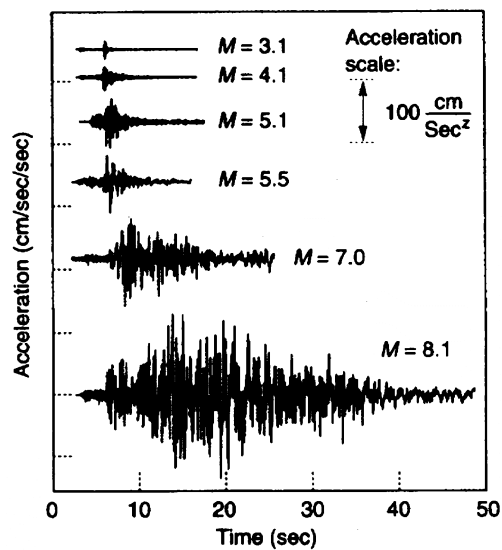
$$a_g(t) = \frac{1}{2\pi} \int_{-\infty}^{\infty} F(\omega) e^{i\omega t} d\omega$$

Sample Fourier amplitude spectra of ground motions recorded at two adjacent sites during the 1989 Loma Prieta earthquake are shown below. What can be gleaned from these two figures?



5.3.2 Duration of Strong Motion Shaking

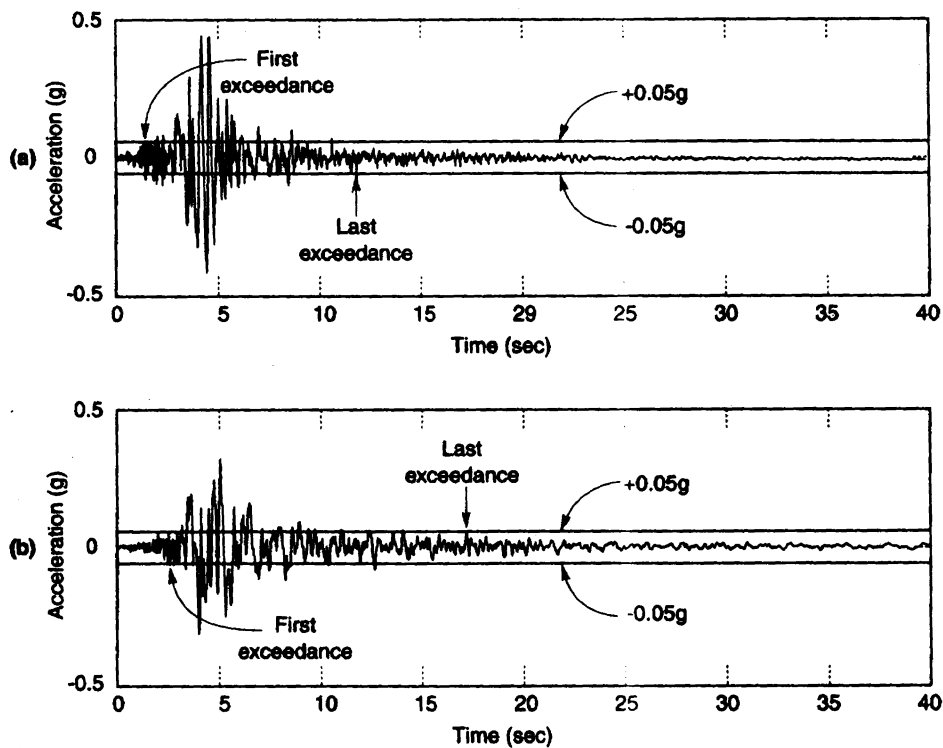
The *duration* of an earthquake history is somewhat dependent on the magnitude of the earthquake. Consider the figure below from Kramer that shows accelerograms from six earthquakes off the Pacific coast of Mexico. The epicentral distance was the same for all six earthquakes. What do you conclude from the information presented in the figure?



The duration of strong-motion shaking plays a role in the response of nonlinear components and systems that are subject to cumulative damage and stiffness and strength degradation.

A number of definitions of strong-motion duration have been proposed including

- *Bracketed duration*: the time between the first and last crossing of threshold acceleration (e.g., 0.05g). This definition was provided by Bolt in 1973. The figure at the top of the following page illustrates how the bracketed duration is calculated.
- *Significant duration*: the time variation of the integral of the square of the ground acceleration history. This definition is related to the Arias intensity. Two common definitions are the time intervals between 5% and 95% (Trifunac and Brady, 1975) and 5% and 75% (Stewart et al. 2001) of the integral of the square of the ground acceleration. The second figure on the previous page illustrates the Trifunac and Brady calculation.



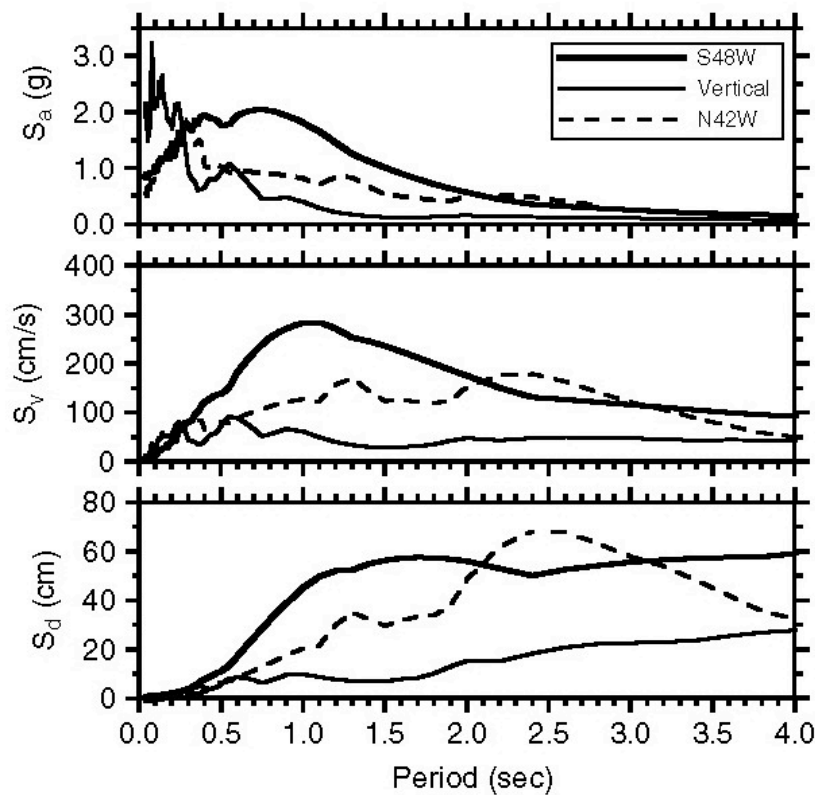
6. Characterizing Earthquake Ground Motions Using Elastic Spectra

Elastic response spectra have been widely used in earthquake engineering for 40+ years in the United States. Spectra were originally developed by Biot (1933) and Housner (1941) to present the maximum response over time of a linear single-degree-of-freedom oscillator versus its natural period (or frequency) subjected to a base ground-motion history. Spectral information is

generally presented in a *linear-linear* format but *log-log* and *tripartite* formats are popular in some industries (e.g., nuclear power industry). Traditional spectral representations include

- Pseudo acceleration versus natural period (frequency)
- Pseudo velocity versus natural period (frequency)
- Spectral displacement versus natural period (frequency)

For example, pseudo-acceleration, pseudo-velocity and relative displacement spectra generated for 5% damping and the earthquake histories recorded at the Rinaldi Receiving Station during the 1994 Northridge earthquake are shown below (from Bozorgnia and Bertero, 2004).



- Why is 5% damping used to construct the spectra?
- Compare the horizontal spectral ordinates.
- Compare the vertical and horizontal spectra ordinates.

7. Attenuation Relationships

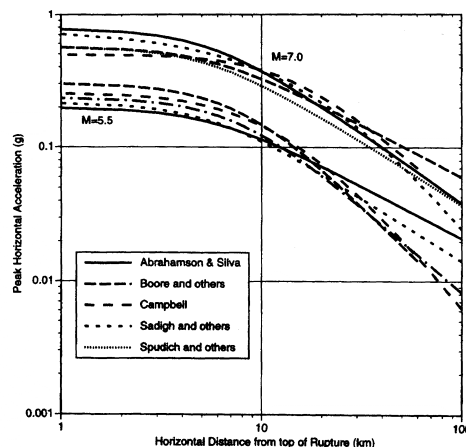
7.1 Introduction

Attenuation relationships relate ground motion parameters to the magnitude of an earthquake and the distance away from the fault rupture. Relationships have been established for many ground motion parameters including

- Peak horizontal ground acceleration, velocity, displacement and corresponding spectral terms
- Peak vertical ground acceleration, velocity, displacement and corresponding spectral terms

7.2 Attenuation Relationships

Attenuation relationships are developed by statistical evaluation of large sets of ground motion data. Relationships have been developed for different regions of the United States (and other countries), different fault types (strike-slip, dip-slip and subduction). These relationships are only as good as the dataset from which the relationships were derived; the greater the size of the data set, the more robust the relationship. A set of attenuation relationships, which plot peak horizontal acceleration versus distance in a log-log scale is presented below. What information is presented here?



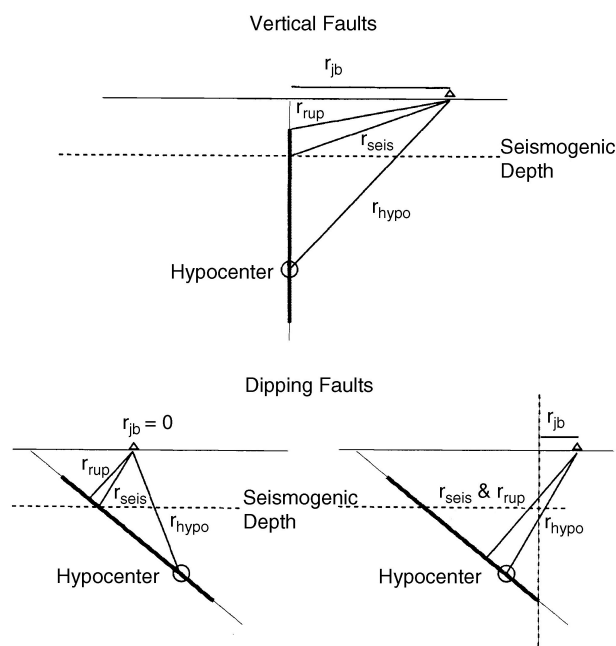
In its most basic form, the attenuation relationship can be described by an equation of the form

$$\ln Y = c_1 + c_2 M - c_3 \ln R - c_4 R + \varepsilon$$

where $\ln Y$ is the natural logarithm of the strong-motion parameter of interest (e.g., peak ground acceleration, spectral horizontal acceleration), M is the earthquake magnitude, R is the source-to-site distance or a term characterizing this distance, and ε is the standard error term with a mean of zero and a standard deviation of $\sigma_{\ln Y}$. The term $c_2 M$ is consistent with the definition of earthquake magnitude (the *source*) as a logarithmic measure of the amplitude of the ground motion. The term $-c_3 \ln R$ (the *path*) is consistent with the geometric spread of the seismic wave

front as it propagates from the source. The value of c_3 will vary with distance depending on the seismic wave type (body wave, surface wave, etc). The term $-c_4R$ is consistent with the anelastic attenuation of seismic waves caused by material damping (treating soil as a viscoelastic materials) and scattering (a result of reflections and refractions of seismic waves due to the presence of heterogeneities and discontinuities in the earth's crust, causing multiple seismic waves to arrive at a site from different paths of differing lengths). Typical attenuation relationships are more complicated than the basic equation given above. Additional terms are needed to account for other effects including near-source directivity, faulting mechanism (strike slip, reverse and normal), site conditions (different relationships), and hanging wall/footwall location of the site.

All of the ground motion attenuation relationships described in this module use moment magnitude M_w to define earthquake magnitude. Attenuation relationships use different definitions of site-to-source distance; some of the definitions are illustrated below in a figure adapted from Abrahamson and Shedlock (1997). (The seismogenic depth is the depth of the surface materials.)



Attenuation relationships are derived using regression analysis on large ground-motion data sets². Regression analysis is used to determine the best estimate of the coefficients in the relationship (i.e., the c_1 through c_4 in the basic attenuation relationship).

² For a given pair of horizontal earthquake histories, the geometric mean (\bar{S}_g of the spectral ordinates of the two components (S_x and S_y)) is generally used to characterize the pair of histories: $\bar{S}_g = \sqrt{S_x S_y}$. Because the functional form of the attenuation relationship involves the

The logarithm of Y is the product of the basic attenuation relationship of Section 9.1. The value predicted by this equation is the mean value of $\ln Y$, or the 50th-percentile or median value of Y . The median value, by definition is exceeded by 50% of the underlying observations. To compute different probabilities of exceedance,

$$\ln Y_{1-\alpha} = \ln Y + z_{\alpha} \sigma_{\ln Y}$$

where z_{α} is the standard normal variable for an exceedance probability of α . When this equation is used to predict ground motion, it is standard practice to employ several attenuation relationships to predict $\ln Y$ to account for epistemic uncertainty (in part).

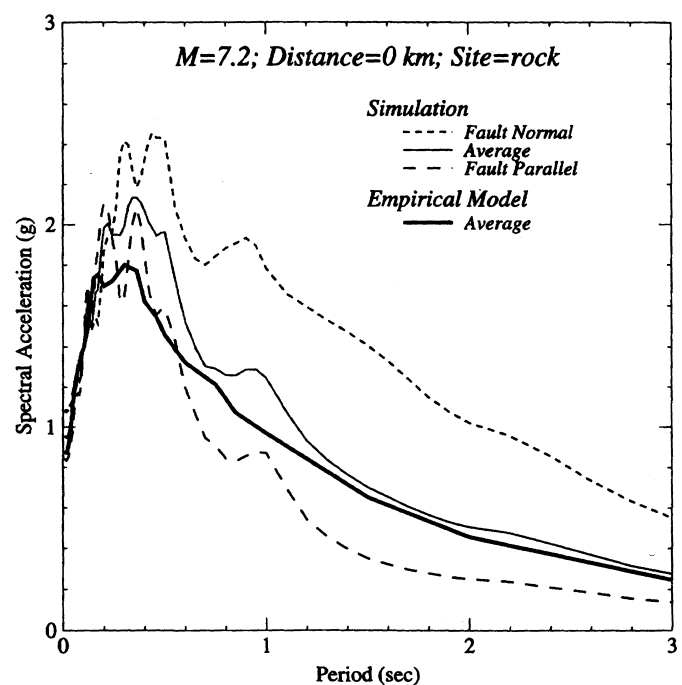
7.3 Modification of Attenuation Relationships for Near-Fault Rupture Directivity

Rupture directivity causes spatial variations in the amplitude and duration of ground motions around faults. Propagation of rupture towards a site produces larger amplitudes of shaking at periods longer than 0.6 second and shorter strong-motion durations than for average directivity conditions.

Somerville et al. (1997) developed modifications to the empirical attenuation relations of Abrahamson and Silva (1997) to account for these variations. The study of Somerville et al. is summarized below.

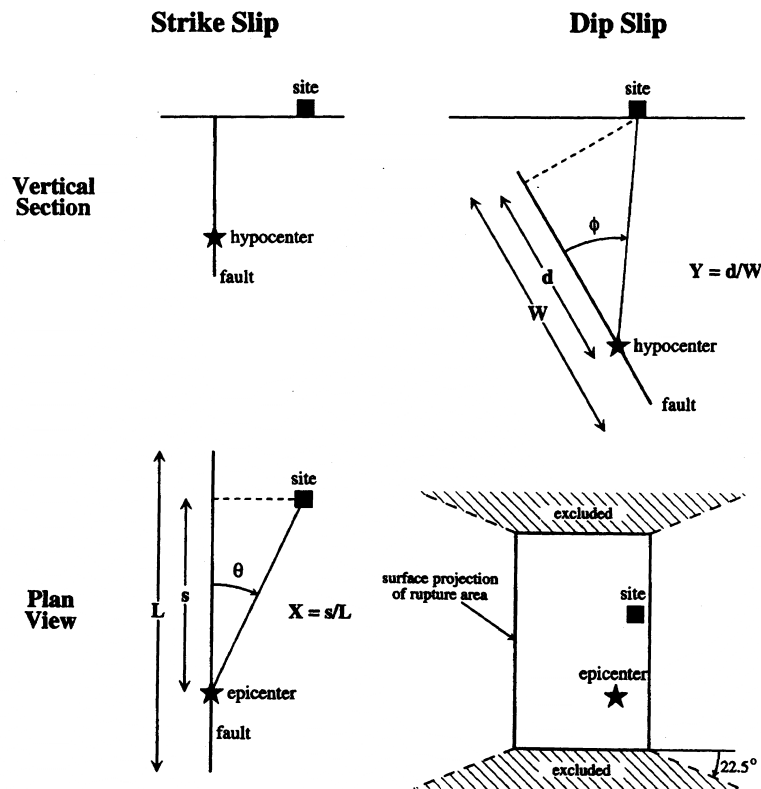
Consider first the figure to the right from Somerville that shows simulations of strike (or fault)-normal and strike-parallel motions directly above a $M7.2$ strike-slip earthquake, and a comparison of their average horizontal motions with the empirical model of Abrahamson and Silva. What are the key observations?

- Average simulation versus average from the empirical model
- Fault normal versus average
- Fault parallel versus average

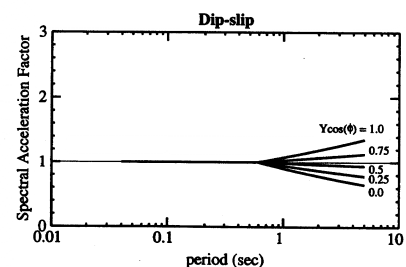
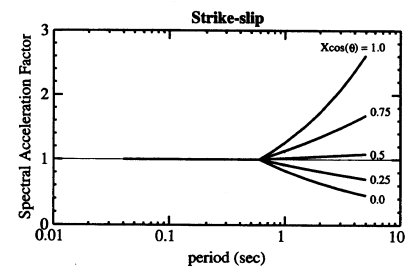


natural log of the ground motion parameter, the geometric mean of the ordinates (which is equivalent to the arithmetic mean of the logs of the ordinates) is used instead of the arithmetic mean.

Fault rupture directivity parameters θ and X for strike-slip faults and ϕ and Y for dip slip faults, and the region off the ends of a dip-slip fault that are excluded from the model are shown below from the paper by Somerville et al. (1997). Somerville considered three ground motion parameters: (1) *Amplitude factor*: bias in average horizontal response spectrum acceleration with respect to Abrahamson and Silva (1997); (2) *Duration factor*: bias in duration of acceleration with respect to Abrahamson and Silva; and (3) *Strike-normal/Average amplitude*: ratio of strike normal to average (directivity) horizontal response spectrum acceleration.



The empirical model of Somerville that shows the spectral amplification factor (parameter 1 above) is shown to the right for strike-slip and dip-slip faults. At a period of 2 seconds for a strike-slip fault, the maximum directivity response is approx. 1.8 times the average response and the minimum directivity response is approx. 0.6 times the average response. These factors are used as multipliers to the spectral ordinates of Abrahamson and Silva (1997) to calculate spectral ordinates for maximum *average* directivity. Somerville et al. (1997) extended the presentation on directivity effects to further consider the ratio of strike-normal to average directivity motions. Two



equations relating strike-normal and average directivity motions were developed: one including magnitude and closest distance, r_{rup} but excluding consideration of the azimuth and zenith angles [ignoring the location of the site with respect to the epicenter], and one including magnitude, closest distance, and azimuth and zenith angles. The coefficients are presented below in a table adapted from Somerville et al. (1997). The reader is referred to the Somerville paper for more information.

Abrahamson (2000) identified aspects of the spatial component of the Somerville et al. (1997) rupture directivity model (parameter 1) that could be improved to make the correction procedure more amenable for probabilistic seismic hazard assessment. Specifically, Abrahamson proposed the following model to incorporate rupture directivity effects:

$$\ln Y_{Dir} = \ln Y + f_1(DR, \xi)T(r_{rup})T(M_w) + f_2(r_{rup}, M_w, \xi)$$

where Y is the average horizontal component of the ground-motion parameter with null directivity effects (the Abrahamson and Silva relationships of 1997) and Y_{Dir} is the value of Y accounting for rupture directivity effects; $f_1(\cdot)$ accounts for the spatial variability and $f_2(\cdot)$ accounts for orientation with respect to the strike of the fault.

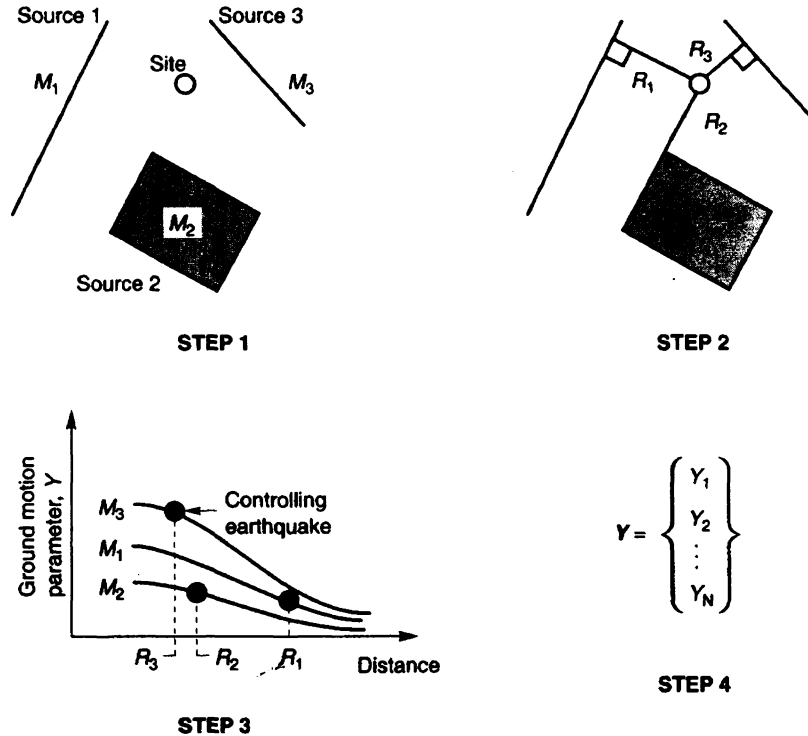
8. Seismic Hazard Analysis

8.1 Introduction

Seismic hazard analysis makes use of the attenuation relationships described above and takes one of two forms: Deterministic Seismic Hazard Analysis (DSHA) and Probabilistic Seismic Hazard Analysis (PSHA). Each type of analysis is described below. Much additional information is provided in Kramer (1996) and McGuire (2004).

8.2 Deterministic Seismic Hazard Analysis (DSHA)

DSHA preceded PSHA as the prevalent form of hazard assessment for maximum (worst case) earthquake shaking. It involves development of a seismic scenario and characterization of that scenario. Kramer describes DSHA as a simple four-step process as enumerated and depicted below. The schematic is from Kramer.



1. *Identify and characterize* (geometry and potential [M_W]) all earthquake sources capable of generating significant shaking at the site. See the figure above in which three sources are shown surrounding the site.
2. Calculate the *source-to-site* distance for each source identified in step 1. Distance measures can include epicentral distance and hypocentral distance: depending on the distance measure adopted in the predictive (attenuation) relationship. Step 2 in the figure below illustrates the calculation.
3. Select the *controlling earthquake*, that is, the earthquake that generates the greatest shaking effect (typically acceleration) at the site using attenuation relationships. Step 3 of the figure illustrates the process for the three sources and distances. The controlling earthquake is described in terms of its magnitude and distance from the site (e.g., M_W 7 at 10 km).
4. Define the hazard at the site by the controlling earthquake (spectral ordinates, maximum ground acceleration, maximum ground velocity, maximum ground displacement).

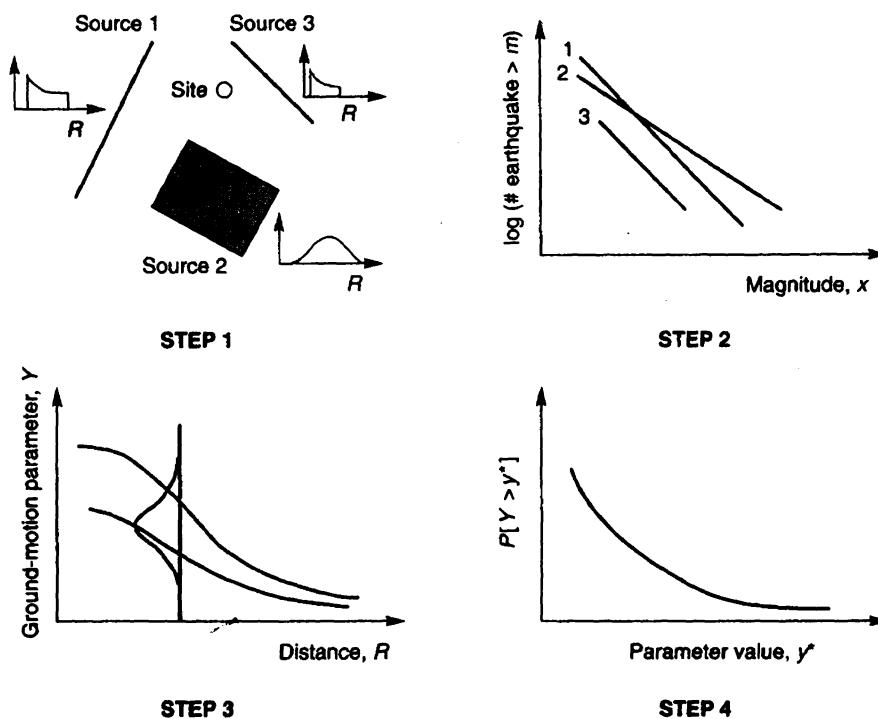
DSHA has the advantage of being simple to apply. The procedure is often conservative where the tectonic features are well defined (line sources) such as the San Andreas and Hayward faults in California. In DSHA, the maximum earthquake assumed to occur at point on fault closest to the site. The shortcomings of DSHA include a) difficult to apply to distributed sources close to the site; what distance should be used?; how should distributed sources far from the site be

treated?; b) uncertainty is not treated well; c) no information is provided on the likelihood of the controlling earthquake; and d) no information is provided on the level of shaking that might be experienced in the lifespan of the structure at the site. Uncertainty can be incorporated into the DSHA calculation by incorporating rudimentary statistics into the calculation by taking one standard deviation above the median at every step in the process (magnitude, PGA, etc); an approach that can lead to large (and perhaps unrealistic) results.

8.3 Probabilistic Seismic Hazard Analysis (PSHA)

8.3.1 Introduction

PSHA rectifies a number of the problems inherent in DSHA by quantifying uncertainty and the probability of earthquake occurrence. As noted by Kramer, PSHA follows similar steps to DSHA but uncertainty is quantified by a probability distribution at every step in the process. Probability distributions are determined for the magnitude of each earthquake on each source, $f_M(m)$, the location of the earthquake in or along each source, $f_R(r)$, and the prediction of the response parameter of interest $P(\text{pga} > \text{pga}' | m, r)$. Kramer describes PSHA as a four-step process as enumerated and depicted below. The schematic is from Kramer.



1. *Identify and characterize* (geometry and potential [M_W]) all earthquake sources capable of generating significant shaking at the site. See the figure above in which three sources are shown surrounding the site. For each source, develop the probability distribution of rupture locations within the source. [A uniform probability distribution is generally chosen, which means that earthquakes are equally likely of occurring at any point along or in the source.]

Combine these distributions with the source geometry to obtain the probability distribution of source-to-site distance. [Contrast this with DSHA that assumes that the probability of occurrence is 1 at the points in each source zone closest to the site and 0 elsewhere.]

2. Develop a seismicity or temporal distribution of earthquake occurrence. A recurrence relationship, which specifies the average rate at which an earthquake of some size will be exceeded, is used to characterize the seismicity of each source zone. [The recurrence relationship may accommodate the maximum earthquake but is not limited to that earthquake, as DSHA often does.]
3. The ground motion produced at the site by earthquakes of any possible size (magnitude) occurring at any possible point in each source zone must be determined with the use of predictive (attenuation) relationships. [The uncertainty inherent in the attenuation relationship is also considered explicitly in PSHA unlike DSHA.]
4. The uncertainties in earthquake location, size, and ground motion prediction are combined to obtain the probability that the ground motion parameter (e.g., PHA, spectral acceleration) will be exceeded in a particular time period (say 10% in 50 years).

Summary information on the components of PSHA is presented below. See Kramer (1996), McGuire (2004) and Bozorgnia and Bertero (2004) for more details.

8.3.2 Earthquake Source Characterization

The characterization of an earthquake source (and there might be a number of sources for a given site) requires consideration of the spatial characteristics of the source, the distribution of earthquakes within that source, of the distribution of earthquake size within that source, and of the distribution of earthquakes with time. Each of these characteristics involves some degree of uncertainty (and such uncertainty can be addressed with PSHA).

Spatial Uncertainty

The geometries of earthquake sources are typically characterized as *point sources* (e.g., volcanoes), two-dimensional *areal sources* (e.g., a well-defined fault plane) and three-dimensional *volumetric sources* (e.g., areas where earthquake mechanisms are poorly defined such as the Central and Eastern USA). Source zones might be similar to or different from the actual source, depending on the relative geometry of the source and the site of interest, as shown in the figure below from Kramer.

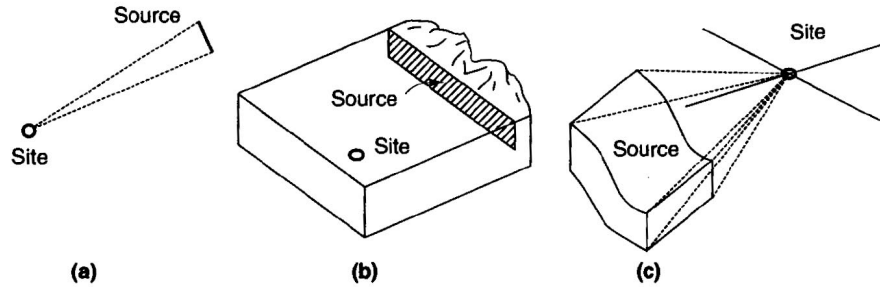


Figure 4.7 Examples of different source zone geometries: (a) short fault that can be modeled as a point source; (b) shallow fault that can be modeled as a linear source; (c) three-dimensional source zone.

Since predictive relationships (such as attenuation relationships) express ground motion parameters in terms of a measure of the source-to-site distance, the spatial uncertainty must be described with respect to the appropriate distance parameter. The uncertainty in source-to-site distance can be described by a probability density function (pdf). Consider the figure below from Kramer.

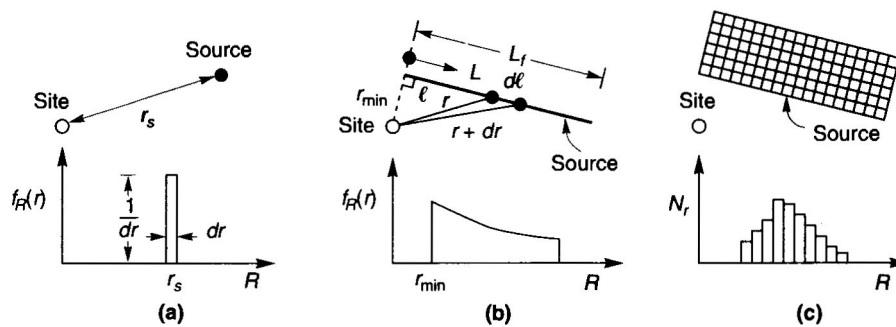


Figure 4.8 Examples of variations of source-to-site distance for different source zone geometries. The shape of the probability distribution can be visualized by considering the relative portions of the source zone that would fall between each of a series of circles (or spheres for three-dimensional problems) with equal differences in radius.

For the point source above, the distance R is r_s and the probability that $R = r_s$ is 1.0 and $R \neq r_s$ is 0. For the linear source of part b. of the figure, the probability that an earthquake occurs on small segment of the fault between $L = l$ and $L = l + dl$ is the same as the probability that it occurs between $R = r$ and $R = r + dr$, namely,

$$f_L(l)dl = f_R(r)dr$$

where $f_L(l)$ and $f_R(r)$ are the pdfs for the distance variables L and R , respectively. As a result,

$$f_R(r) = f_L(l) \frac{dl}{dr}$$

If earthquakes are assumed to be uniformly distributed over the length of the fault, $f_L(l) = 1/L_f$. Since $l^2 = r^2 - r_{\min}^2$, the pdf of R is given by

$$f_R(r) = \frac{r}{L_f \sqrt{r^2 - r_{\min}^2}}$$

For more complex source zones, it is easier to evaluate $f_R(r)$ by numerical integration. For example, the source zone of part c. of the figure above is broken up into a large number of discrete elements of the same area. A histogram that approximates $f_R(r)$ can be constructed by tabulating the values of R that correspond to the center of each element.

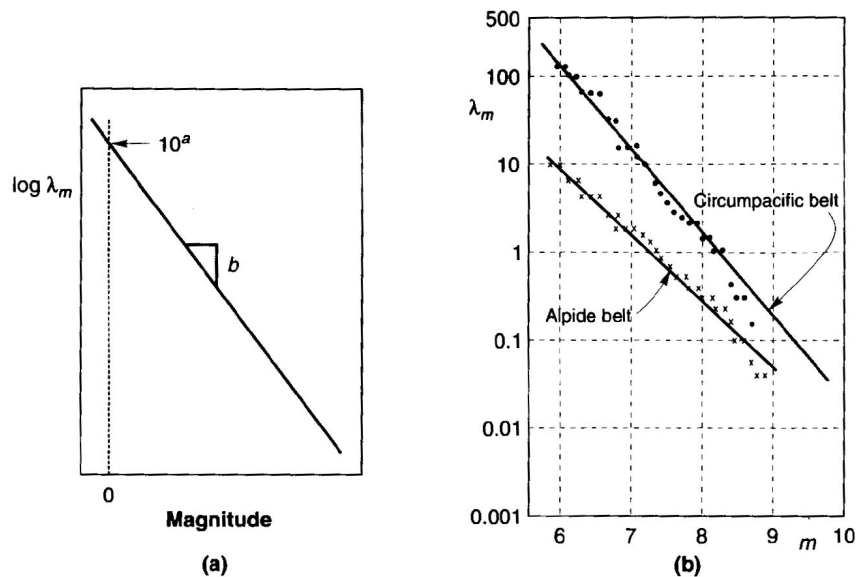
Size Uncertainty

The distribution of earthquake sizes in a given period is described by a *recurrence law*. One basic assumption of PSHA is that the recurrence law obtained on the basis of past seismicity is appropriate for the prediction of future seismicity. The best known recurrence law is that of Gutenberg and Richter (1944), who collected data from Southern Californian earthquakes over a period of years and plotted the data according to the number of earthquakes that exceeded different magnitudes during that period. The number of exceedances of each magnitude was divided by the length of the time period used to assemble the data to define a *mean annual rate of exceedance* λ_m of an earthquake of magnitude m . The reciprocal of the mean annual rate of exceedance of a particular magnitude is termed the return period of earthquakes exceeding that magnitude. G-R plotted the logarithm of the annual rate of exceedance (of earthquakes in Southern California) against earthquake magnitude and the resulting relationship was linear, namely,

$$\log_{10} \lambda_m = a - bm$$

where λ_m is defined above, 10^a is the mean yearly number of earthquakes of magnitude greater than or equal to 0, and b describes the relative likelihood of large and small earthquakes. As the value of b increases, the number of larger magnitude earthquakes relative to smaller magnitude earthquakes decreases. The values of a and b are generally obtained by regression analysis on a database of seismicity from the source zone of interest. (The mean rate of small earthquakes is often underpredicted because historical records are often used to supplement the instrumental records and only the larger magnitude events from part of the historical record.) The figure below from Kramer illustrates the equation; worldwide recurrence data is shown in part b. of the figure.

- How are historical records used to estimate magnitude? Conversion of size data to magnitude?



The G-R recurrence law can also be expressed as

$$\lambda_m = 10^{a-bm} = \exp(2.303a - 2.303bm)$$

which shows that the G-R law implies that earthquake magnitudes are exponentially distributed and that the range of magnitude is from $-\infty$ to ∞ . Small magnitude earthquakes are of little significance to the built environment and can be ignored in terms of hazard assessment. The G-R law also predicts non-zero mean rates of exceedance from magnitudes up to ∞ , which is not possible. To deal with these practical bounds on magnitude, bounded (lower and upper) recurrence laws have been proposed.

The PDF and CDF for the G-R law with upper and lower bounds, m_u and m_0 , respectively, are

$$f_M(m) = \frac{\beta e^{-\beta(m-m_0)}}{1 - e^{-\beta(m_u-m_0)}}$$

$$F_M(m) = P[M < m \mid m_0 \leq m \leq m_u] = \frac{1 - e^{-\beta(m-m_0)}}{1 - e^{-\beta(m_u-m_0)}}$$

where $\beta = 2.303b$.

The G-R law was originally developed from regional data and not for specific source zones. Paleoseismic studies over the past 30 years have indicated that individual points on faults (or fault segments) tend to move by approximately the same distance in each earthquakes, suggesting that individual faults repeatedly generate earthquakes of a similar (with 0.5 magnitude unit) size, known as *characteristic earthquakes* at or near their maximum magnitude. Geological evidence indicates that characteristic earthquakes occur more frequently than that

would be implied by extrapolation of the G-R law from high exceedance rates (of low magnitude events) to low exceedance rates (of high magnitude).

Predictive Relationships

As noted previously, predictive relationships are generally obtained empirically by least-squares regression on a strong-motion dataset. Scatter (randomness) in the results is inevitable for reasons that have identified earlier, namely,

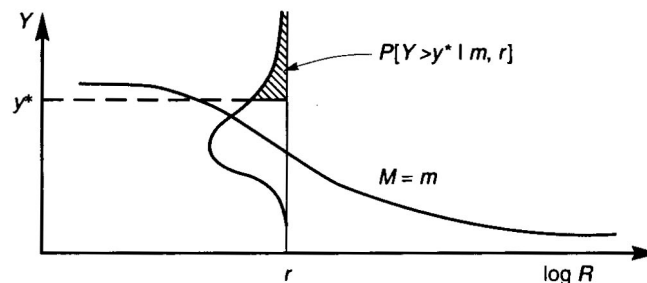
- Rupture mechanics
- Travel path
- Site conditions

(The scatter can be characterized by confidence limits or by the standard deviation of the predicted parameter.)

The probability that a ground motion parameter Y exceeds a certain value y for an earthquake of magnitude m , occurring at a distance r is given by

$$P[Y > y | m, r] = 1 - F_Y(y)$$

where $F_Y(y)$ is the value of the CDF of Y at m and r . The value of $F_Y(y)$ depends on the probability distribution used to describe Y . As noted previously, ground motion parameters are generally assumed to be lognormally distributed. The figure below from Kramer illustrates the conditional probability of exceeding a particular value of a ground motion parameter for a given combination of m and r .



Temporal Uncertainty

The distribution of earthquake occurrence with time must be computed or assumed to calculate the probabilities of different earthquake magnitudes occurring in a given time period. Earthquakes are assumed to occur randomly with time and the assumption of random occurrence permits the use of simple probability models.

The temporal occurrence of earthquakes is commonly described as a *Poisson* process: one that yields values of a random variable describing the number of occurrences of a particular event

during a given time interval (or spatial region). In a Poisson process, a) the number of occurrences in one time interval are independent of the number that occur in any other time interval; b) the probability of occurrence during a very short time interval is proportional to the length of the time interval; and c) the probability of more than one occurrence in a very short time interval is negligible. Events in a Poisson process occur randomly, with no memory of the time, size or location of any preceding events.

For a Poisson process, the probability of a random variable N , representing the number of occurrences of a particular event in a given time period is given by

$$P[N = n] = \frac{\mu^n e^{-\mu}}{n!}$$

where μ is the average number of occurrences of the event in the time period. To characterize the temporal distribution of earthquake recurrence for PSHA, the Poisson probability is normally expressed as

$$P[N = n] = \frac{(\lambda t)^n e^{-\lambda t}}{n!}$$

where λ is the average rate of recurrence of the event and t is the time period. When the event is the exceedance of a particular earthquake magnitude, the Poisson model can be combined with a suitable recurrence law to predict the probability of at least one exceedance in a period of t years by³

$$P[N \geq 1] = 1 - e^{-\lambda t}$$

Probability Computations and Seismic Hazard Curves

The development of *seismic hazard curves*, which indicate the annual probability of exceedance of different values of a selected ground motion parameter, involves probabilistic calculations that combine the uncertainties in earthquake size, location and frequency for each potential earthquake source that could impact shaking at the site under study. The seismic hazard curves can then be used to compute the probability of exceeding the chosen ground motion parameter in a specified period of time.

The seismic hazard curve calculations are (somewhat) straightforward once the uncertainties in earthquake size, location and frequency are established but much bookkeeping is involved. The probability of exceeding a particular value y of a ground motion parameter Y is calculated for one

³ The probability of at least one exceedance in a given time period t is given by

$$P[N \geq 1] = P[N = 1] + P[N = 2] + \dots + P[N = \infty] = 1 - P[N = 0] = 1 - e^{-\lambda t}$$

possible source location and then multiplied by the probability of that magnitude earthquake occurring at that particular location. The calculation is then repeated for all possible magnitudes and locations and the probabilities of each are summed to compute the $P[Y > y]$ at the site. Calculations from Kramer (1996) are summarized and reproduced below.

For a given earthquake occurrence, the probability that a ground motion parameter Y will exceed a particular value y^* can be computed using the total probability theorem (Cornell and Benjamin), namely,

$$P[Y > y^*] = P[Y > y^* | \mathbf{X}] P[\mathbf{X}] = \int P[Y > y^* | \mathbf{X}] f_{\mathbf{x}}(\mathbf{X}) dx$$

where \mathbf{X} is a vector of random variables that influence Y . In most cases, the quantities in \mathbf{X} are limited to the magnitude M and distance R . Assuming that M and R are independent, the probability of exceedance can be written as

$$P[Y > y^*] = \iint P[Y > y^* | m, r] f_M(m) f_R(r) dm dr$$

where $P[Y > y^* | m, r]$ is obtained from the predictive relationship and $f_M(m)$ and $f_R(r)$ are the pdfs for magnitude and distance, respectively.

If the site under study is in a region of N_s potential earthquake sources, each of which has an average rate of threshold exceedance $\nu_i = \exp(\alpha_i - \beta_i m)$, the total average exceedance rate for the region is given by the equation below, which is typically solved by numerical integration.

$$\lambda_{y^*} = \sum_{i=1}^{N_s} \nu_i \iint P[Y > y^* | m, r] f_{M_i}(m) f_{R_i}(r) dm dr$$

One approach that is described by Kramer (as simple rather than efficient) is to divide the possible ranges of magnitude and distance into N_M and N_R segments, respectively. The average exceedance rate can then be calculated using a multi-level summation as follows:

$$\begin{aligned} \lambda_{y^*} &= \sum_{i=1}^{N_s} \sum_{j=1}^{N_M} \sum_{k=1}^{N_R} \nu_i P[Y > y^* | m_j, r_k] f_{M_i}(m_j) f_{R_i}(r_k) \Delta m \Delta r \\ &= \sum_{i=1}^{N_s} \sum_{j=1}^{N_M} \sum_{k=1}^{N_R} \nu_i P[Y > y^* | m_j, r_k] P[M = m_j] P[R = r_k] \end{aligned}$$

where the terms are $m_j = m_0 + (j - 0.5)(m_{\max} - m_0) / N_M$, $r_k = r_{\min} + (k - 0.5)(r_{\max} - r_{\min}) / N_R$, $\Delta m = (m_{\max} - m_0) / N_M$ and $\Delta r = (r_{\max} - r_{\min}) / N_R$. The above statement is equivalent to assuming that each source is capable of generating only N_M different earthquakes of magnitude m_j at only N_R different source-to-site distances of r_k . The accuracy of the above method increases with smaller segments and thus larger values of N_M and N_R .

A sample seismic hazard curve is shown below. What spectral demands are presented here?

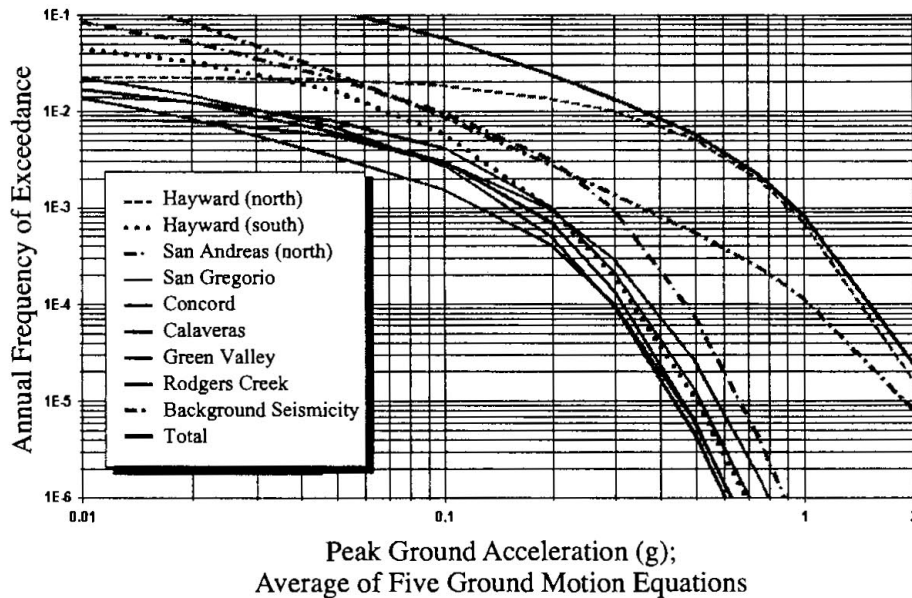


Figure 29. Contribution to the PGA hazard in Berkeley, for each fault and background seismicity.

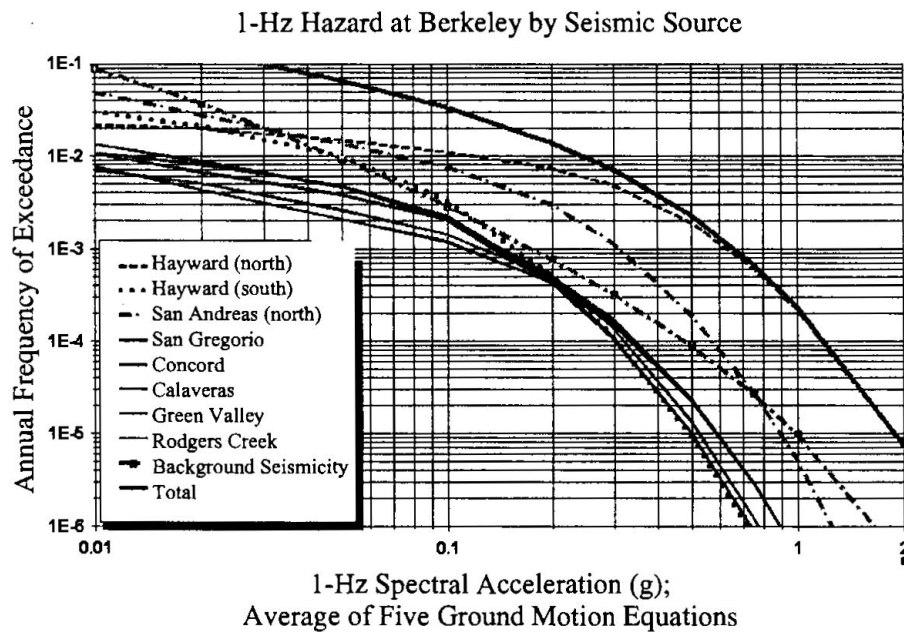


Figure 30. Contribution to the 1-Hz SA hazard in Berkeley, for each fault and background seismicity.

Computations for Finite Time Periods

Probabilities of exceedance in a selected time period can be computed using seismic hazard curves combined with the Poisson model. From before, the probability of exceedance of y in a time period T is

$$P[Y_T > y] = 1 - e^{-\lambda_y T}$$

As an example, we compute the probability that a peak horizontal acceleration of 0.10g would be exceeded in a 50-year time period for the site characterized by the hazard curve above:

$$P[\text{PHA} > 0.1g \text{ in } 50 \text{ years}] = 1 - e^{-\lambda_y T} = 1 - e^{-(0.06)(50)} = 0.95 = 95\%$$

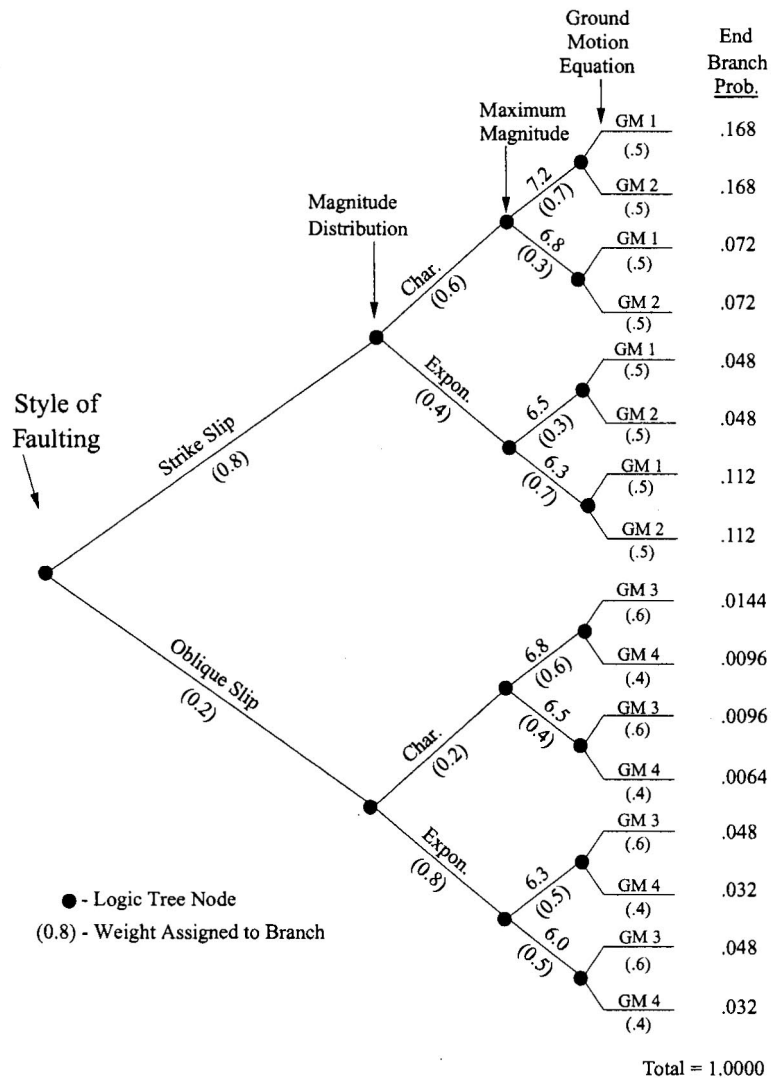
An alternate, often made, computation is the value of the ground motion parameter corresponding to a particular probability of exceedance in a given time period. For example, the acceleration that has a 10% probability of exceedance in a 50-year period would be that with an annual rate of exceedance, calculated by re-arranging the second-to-last equation, namely

$$\lambda_y = -\frac{\ln(1 - P[Y_T > y])}{T} = \frac{\ln(1 - 0.10)}{50} = 0.00211$$

Treatment of Model Uncertainty

The computations presented above provide a systematic framework for the treatment of uncertainty in the values of the parameters of a particular seismic hazard model. However, the best choices for elements of the hazard model are themselves uncertain and the use of logic trees provides a convenient framework for the explicit treatment of model uncertainty. A sample logic tree from McGuire (2004) is presented on the following page for a single source zone. The ground motion equation in this figure is equivalent to the attenuation relationships described previously. The Expon in the figure refers to the G-R model (or bounded derivative thereof).

In the logic tree, each alternative model is assigned a weighting factor that can be interpreted as the relative likelihood of that model being correct. The tree consists of a series of nodes, points at which models are specified and branches that represent the different models under consideration. The sum of the probabilities of all branches connected to a given node must be 1.0 as indicated in the figure. In this tree, which is developed for one source zone (of which there might be many for a given site), uncertainty in the style of faulting, magnitude distribution (characteristic versus exponential [G-R]), maximum magnitude, and attenuation relationship are considered. This logic tree terminates with 16 branches, each with its own weighting. To use a logic tree, the hazard analysis is carried out for each combination of models associated with a terminal branch. The result of each analysis is then weighted by the relative likelihood of its combination of branches. The final result is the sum of the weighted individual results.



Near-Field Effects and Probabilistic Seismic Hazard Assessment

Near-field effects can be directly included in the development of seismic hazard curves using the attenuation relationships of Abrahamson (2000) that were described previously.

9. Hazard Characterization per the 2003 NEHRP Recommended Provisions

9.1 Introduction

The 2003 *NEHRP Recommended Provisions* provides a simple strategy for estimating the maximum and design earthquake hazard. The product of the calculation is a *median* estimate of the spectral demands. Standard spectral shapes and mapped values of spectral acceleration at 0.2 second and 1.0 second are used to characterize the elastic design response spectrum. These *NEHRP Recommended Provisions* use the USGS probabilistic seismic hazard maps (the latest edition is 2002) as the basis for hazard computations. Visit <http://eqhazmaps.usgs.gov/> for

details. Maps are provided for return periods of 475 years (10% probability of exceedance in 50 years) and 2475 years (2% probability of exceedance in 50 years).

Spectral demands are computed at 0.2 second (short period, S_s , constant acceleration range) and 1.0 second (long period, S_1 , constant velocity range). The period of 0.2 second was chosen for the definition of the short-period acceleration S_s because in the central and eastern United States, the spectral acceleration at 0.2 second is larger than that at 0.3 second and better quantifies the short-period demands. In the western United States there is little difference between the 0.2- second and 0.3-second spectral ordinates.

9.2 General Procedure for Characterizing the Maximum Earthquake

Maximum earthquake shaking is defined for a uniform probability of exceedance of 2% in 50 years. The maximum earthquake is characterized first for a rock site and then modified to account for local soil effects. The rock-site characterization is based on spectral accelerations at 0.2 second (S_s) and 1.0 second (S_1) per the USGS maps. The maximum earthquake spectral response accelerations for short periods (S_{MS}) and at 1 second (S_{M1}) are then adjusted for site effects as follows

$$S_{MS} = F_a S_s \quad \text{and} \quad S_{M1} = F_v S_1$$

where site coefficients F_a and F_v are defined in Section 4 of the 2003 *NEHRP Recommended Provisions*. Values of these coefficients vary as a function of S_s and S_1 and soil type (A through F) as shown in the tables below that are extracted from the *Provisions*. Consider the range of values for the soil multipliers? Why is the range so large? Note that a cap is set on the probabilistically based NEHRP spectrum through the use of a deterministic spectrum that is explained in Bozorgnia and Bertero (2004).

Table 3.3-1 Values of Site Coefficient F_a

Site Class	Mapped MCE Spectral Response Acceleration Parameter at 0.2 Second Period ^a				
	$S_s \leq 0.25$	$S_s = 0.50$	$S_s = 0.75$	$S_s = 1.00$	$S_s \geq 1.25$
A	0.8	0.8	0.8	0.8	0.8
B	1.0	1.0	1.0	1.0	1.0
C	1.2	1.2	1.1	1.0	1.0
D	1.6	1.4	1.2	1.1	1.0
E	2.5	1.7	1.2	0.9	0.9
F	— ^b	— ^b	— ^b	— ^b	— ^b

^a Use straight line interpolation for intermediate values of S_s .
^b Site-specific geotechnical investigation and dynamic site response analyses shall be performed.

Table 3.3-2 Values of Site Coefficient F_v

Site Class	Mapped MCE Spectral Response Acceleration Parameter at 1 Second Period ^a				
	$S_I \leq 0.1$	$S_I = 0.2$	$S_I = 0.3$	$S_I = 0.4$	$S_I \geq 0.5$
A	0.8	0.8	0.8	0.8	0.8
B	1.0	1.0	1.0	1.0	1.0
C	1.7	1.6	1.5	1.4	1.3
D	2.4	2.0	1.8	1.6	1.5
E	3.5	3.2	2.8	2.4	2.4
F	— ^b	— ^b	— ^b	— ^b	— ^b

^a Use straight line interpolation for intermediate values of S_I .
^b Site-specific geotechnical investigation and dynamic site response analyses shall be performed.

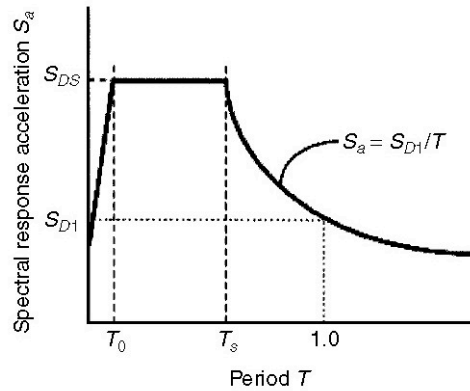
9.3 General Procedure for Characterizing the Design Earthquake

In editions of the *NEHRP Recommended Provisions* prior to 2000, the *design* earthquake was characterized by a return period of 475 years. This characterization changed in the 2000 *NEHRP Recommended Provisions* wherein the design earthquake spectral ordinates were determined as follows unless a site-specific hazard analysis was undertaken. In the 2000 *NEHRP Recommended Provisions*, the design earthquake response accelerations were determined as follows

$$S_{DS} = \frac{S_{MS}}{1.5} = \frac{F_a S_s}{1.5} \quad \text{and} \quad S_{DI} = \frac{S_{M1}}{1.5} = \frac{F_v S_1}{1.5}$$

An identical approach is used in the 2003 *NEHRP Recommended Provisions* for characterizing the design earthquake. The figure below shows the shape of the *design* earthquake spectrum.

In this figure, the design earthquake ordinates, S_{DS} and S_{DI} , completely define the spectrum. The period T_S is the corner period in the spectrum and T_0 is defined as 20 percent of T_S .



In this figure, the design earthquake ordinates, S_{DS} and S_{D1} , completely define the spectrum. The period T_s is the corner period in the spectrum and T_0 is defined as 20 percent of T_s .

10. New Seismic Hazard Representations in ASCE-7-10

ASCE-7-10 (and the 2009 *NEHRP Recommended Provisions*) will include new definitions of seismic hazard for the design of structures

- Spectrum for maximum-direction ground motion
- 84% maximum-direction deterministic limit on the results of PSHA
- Pairs of earthquake histories to recover the geomean horizontal spectrum

- End -